AD_____

Award Number: DAMD17-00-1-0577

TITLE: Biomechanical Studies and Optical Digitizer Development for Enhanced Orthopedic Footware

PRINCIPAL INVESTIGATOR: Vern L. Houston, Ph.D.

CONTRACTING ORGANIZATION: Veterans Administration New York Harbor Healthcare System
New York, New York 10010

REPORT DATE: September 2002

TYPE OF REPORT: Annual

PREPARED FOR: U.S. Army Medical Research and Materiel Command
Fort Detrick, Maryland 21702-5012

DISTRIBUTION STATEMENT: Approved for Public Release;
Distribution Unlimited

The views, opinions and/or findings contained in this report are those of the author(s) and should not be construed as an official Department of the Army position, policy or decision unless so designated by other documentation.

REPORT DOCUMENTATION PAGE

Form Approved
OMB No. 074-0188

1. AGENCY USE ONLY (Leave blank)	2. REPORT DATE	3. REPORT TYPE AND DATES COVERED
	September 2002	Annual (15 Aug 01 - 15 Aug 02)

4. TITLE AND SUBTITLE
Biomechanical Studies and Optical Digitizer Development for Enhanced Orthopedic Footware

5. FUNDING NUMBERS
DAMD17-00-1-0577

6. AUTHOR(S) :
Vern L. Houston, Ph.D.

7. PERFORMING ORGANIZATION NAME(S) AND ADDRESS(ES)
Veterans Administration New York Harbor
Healthcare System
New York, New York 10010

E-Mail: vlh3@nyu.edu

8. PERFORMING ORGANIZATION REPORT NUMBER

9. SPONSORING / MONITORING AGENCY NAME(S) AND ADDRESS(ES)
U.S. Army Medical Research and Materiel Command
Fort Detrick, Maryland 21702-5012

10. SPONSORING / MONITORING AGENCY REPORT NUMBER

11. SUPPLEMENTARY NOTES
Original contains color plates: All DTIC reproductions will be in black and white.

12a. DISTRIBUTION / AVAILABILITY STATEMENT
Approved for Public Release; Distribution Unlimited

12b. DISTRIBUTION CODE

13. Abstract ***(Maximum 200 Words)*** *(abstract should contain no proprietary or confidential information)*

Properly fitting, functional footwear is paramount for preventing foot/ankle discomfort and injury, and maintaining mobility of military personnel and veterans. Custom designed and manufactured orthopedic footwear is an essential component in treatment and rehabilitative care of persons with neuromusculoskeletal foot/ankle pathologies, biomechanical disorders and injuries, and systemic disorders, such as Diabetes Mellitus and peripheral vascular disease, that secondarily affect peoples' feet/ankles. Orthopedic footwear design is still based almost exclusively on pedorthists' subjective judgements, however, so the degree of fit and function attained and quality of footwear produced are highly dependent upon the level of training, experience, and skill of the pedorthist. The objective of this project is to develop quantitative methods for effective, expeditious, repeatable, and consistent design and manufacture of well-fitting, comfortable, and functional orthopedic footwear. To accomplish this a 3-D optical digitizer is being developed capable of rapidly and accurately scanning peoples' feet/ankles in natural and prescribed alignments, in partial and full weight bearing states, with preservation of anatomical fiduciary landmarks' spatial location; together with conduct of biomechanical studies: (i) to derive measures quantifying footwear fit; (ii) to derive quantitative design specifications for footwear orthopedic components and modifications; and (iii) to determine the mechanical characteristics of insole materials.

14. SUBJECT TERMS:
pedorthics, foot, shoes, biomechanics, 3-D digitization, computer-aided design and manufacturing

15. NUMBER OF PAGES
49

16. PRICE CODE

17. SECURITY CLASSIFICATION OF REPORT	18. SECURITY CLASSIFICATION OF THIS PAGE	19. SECURITY CLASSIFICATION OF ABSTRACT	20. LIMITATION OF ABSTRACT
Unclassified	Unclassified	Unclassified	Unlimited

Table of Contents

Introduction — Properly fitting and functioning footwear is essential for prevention of foot and ankle injuries, and for maintaining mobility of military personnel, veterans, and persons in the civilian population. This is especially true for women, who have historically been plagued with foot/ankle problems from ill-fitting footwear. Studies have shown that female military personnel suffer a disproportionately high incidence of musculoskeletal injuries (as high as 10:1) during basic training compared to their male counterparts, and that a principal factor contributing to this high incidence of trauma is ill-fitting, inadequately functioning footwear [Ross and Woodward 1994; Reinker and Ozburne 1979]. In addition to preventing injury, properly fitting and functional footwear is a crucial component in the treatment and rehabilitative care of persons suffering neuromusculoskeletal disorders, and/or systemic diseases, such as Diabetes Mellitus, arthritis, or peripheral vascular disease, with associated secondary complications that affect the feet and ankles [D'Ambrosia 1987; Riddle and Freeman 1988; Rodgers and Cavanagh 1989; Boulton et al. 1993; Boulton 1998; Coleman 1993; Gould 1982; Janisse 1998; Lord and Hosein 1992; Moncur and Shields 1983; Schaff and Cavanagh 1990; Tovey and Moss 1987; Wosk and Voloshin 1985; Mueller 1999; van Schie et al. 2000; Kelly, et al. 2000]. In these cases, well-fitting, functional, comfortable footwear can be the difference between independent, unaided mobility, and forced reliance on crutches, or confinement to a wheelchair, or in the case of diabetic patients with peripheral neuropathy and vascular disease, prevention of pedal ulceration, necrosis, gangrene, and consequent amputation, Figure 1.

Unfortunately, design and manufacture of footwear has remained almost exclusively a subjective, slow, laborious process. Use of quantitative information in pedorthics is quite limited. At most, only a small set of 2-D measurements are used to design and fit footwear (typically just heel-to-toe length and metatarsal ball width). Consequently, design and manufacture of footwear (especially orthopedic footwear) is highly dependent upon the level of training, clinical experience, and skill of the pedorthist(s) involved. More exacting, quantitative measures of pedal geometry, morphology, and biomechanical function, together with more precise, comprehensive, consistent (and automated) methods of design and manufacture, are needed. Although a number of studies have been performed in which foot/shoe plantar interface pressures have been recorded, the work reported has been principally limited to case studies and phenomenological explorations [Mueller, et al. 1994; Schaff 1993; Young 1993; Rose, et al. 1992; Donaghue, et al. 1996]. Few, if any, controlled, quantitative investigations have been conducted from which general principles for design of orthopedic footwear can be formulated, or quantitative specifications for orthopedic footwear components and modifications can be derived. Such research, leading to development of improved equipment and procedures enabling effective, efficient, expeditious, and consistent design and manufacture of better fitting, more functional and comfortable footwear for US military personnel, veterans, and civilians is needed.

The objective of this project is to develop knowledge, equipment, and procedures that will contribute to the quantitative design and manufacture of well-fitting, comfortable, and functional (orthopedic) footwear. A 3-D optical digitizer is being developed that can rapidly, accurately, repeatably and consistently scan peoples' feet and ankles in natural and prescribed orthopedic alignments, in partial and full weight bearing states, registering the spatial location of fiduciary anatomical landmarks. In addition, biomechanical studies are being conducted: (i) to derive measures quantifying footwear fit; (ii) to derive quantitative design specifications for orthopedic footwear components and modifications; and (iii) to characterize the mechanical properties and performance of various insole materials.

Project Research

The project research has been divided into six constituent tasks: (1) Pedorthic Optical Digitizer Development; (2) Quantification of Footwear Fit; (3) Assessment of Military Footwear/Last Fit; (4) Footwear Biomechanical Studies; (5) Footwear Material Mechanical Testing; (6) Summary Analysis and Documentation of Results. Work in each respective area is being conducted concurrently.

Pedorthic Optical Digitizer Development — Specifications for a pedorthic optical digitizer were prepared, estimates were solicited, and a contract for procurement of the requisite components was issued in the first year of the project. The components were received at the beginning of the second year of the project. They were subsequently assembled, calibrated in situ, and laboratory tested with a range of geometric phantoms, Figure 2. Work on development of software for control of the digitizer, and for measurement acquisition, processing, and storage was conducted over the first two years of the project. Development of software for import of scan measurements into the VA Pedorthic CAD/CAM System [Houston, et al. 1998b] for measurement visualization and analysis, and for use in design and fabrication of custom orthopedic footwear was also performed in the second year of the project. The adaptation automatic landmark detection, identification, and registration (ALDIR) software, developed by the investigators for preservation of the spatial locations of fiduciary anatomical landmarks in prosthetics applications, was also adapted and tested in the second project year, Figure 3 [Houston, et al. 1998a]. In addition, clinical tests were performed with the digitizer, scanning the feet and ankles of four experimental subjects, Figure 4, prior to its general deployment. Pedal support platens, shaped to match orthopedic footwear plantar contours, were designed and prototypes fabricated from transparent low refractive index Lucite, in a range of sizes with 0.25 inch, 0.50 inch, and 0.625 inch heel heights, respectively. Laboratory tests measuring the platen's transmissivity and refractivity were performed, and an algorithm for compensation of scan image refraction was developed. Clinical tests with the prototype platens, Figure 5, showed significant corruption of the digitizer camera output signals from spurious intra- and inter- scan head laser light reflections, Figure 6. "Workarounds" to circumvent these problems were developed. Specifically, to minimize errors from multiple reflections of the incident laser signal, the power of the plantar scan head laser was reduced. In addition, black silhouettes of the lateral projected contour of subjects' feet were generated, and placed along the lateral border of each subject's foot before scanning, to minimize corruption of the dorsal camera measurements from multiply reflected laser signals, Figure 7. The lateral and medial scan heads were also offset by four centimeters to minimize cross talk between the scan heads. With the introduction of these "workarounds", good quality, accurate scans of test subjects' feet–ankles were able to be obtained, Figure 8. To more permanently solve these problems, and to obviate the need for the complex "workarounds" developed, a new plantar scan head was ordered, incorporating a different frequency laser with adjustable output power to mitigate multiple reflections, and with bandpass filtered cameras to eliminate interference from cross talk from the medial and lateral scan heads' laser signals. Until the new scan head is received, installed, calibrated, and tested, the "workarounds" developed by the investigators have continued to be employed in application of the digitizer in the other project tasks.

Quantification of Footwear Fit — To establish a reference for quantification of footwear fit, US military footwear Lasts for female personnel, and for male personnel for US military oxford style shoes, were obtained from the Defense Logistics Agency, Defense Personnel Service Center (DLA DPSC). 144 of these Lasts were digitized with the optical digitizer. The resulting measurement files were compiled in the project computerized database, and entered into the Last

Library of the VA Pedorthics CAD/CAM System [Houston, et al. 1998b]. Comparative analysis of the resulting scans for a range of sizes, showed the Lasts to be algebraically scaled, Figure 9. Clinical experience has shown feet of normal, healthy individuals do not algebraically scale by more than ±2 sizes without significant error. The fact that DLA DPSC Lasts are algebraically scaled by more than two sizes is a potential reason that military footwear does not properly fit many soldiers, especially female personnel, thus increasing their susceptibility to foot and ankle trauma during basic training and active duty.

In addition to this work, summary statistics were tabulated from the medical and pedorthic records (including orthopedic Last style and dimensions, shoe modifications and upper patterns) of 290 "representative" pedorthic patients' from the VA National Footwear Center. The resulting data was analyzed in the first project year to establish pedal regions with relative low load tolerance, and increased susceptibility to injury, biomechanical disorders, and pathologies, Table 1.

To measure and quantify pedal/footwear dorsal interface stresses in "well-fitting" versus "ill-fitting" footwear during stance and gait, an Tekscan, Inc. IScan stress measurement system was procured. Calibration and laboratory testing of 27 IScan Model #6910 miniature FVR array transducers, however, failed to yield a single transducer with a sensel array with at least four of the nine elements measurable over the range of pressures expected at the pedal interface. Use of the IScan transducers to measure pedal dorsal stressess, therefore, was abandoned. In their place, Flexiforce single element, FVR transducers were procured, calibrated, and used to measure pedal dorsal interface pressures in synchrony with FScan 960 element FVR transducers measuring pedal plantar pressures, in "well-fitting," and in "ill-fitting," footwear during stance and gait, Figure 10. Collection and analysis of this data is continuing.

Assessment of Military Footwear Fit —

To assess the fit of footwear for female military personnel, 43 normal, healthy subjects of military service age were recruited, and casts and scans, together with a set of 23 manual measurements, were acquired of their feet and ankles, Table 2. The parameters measured in the optical scans and those recorded manually comprise the metrics most commonly used in pedorthic Last grading, together with the principal pedal dimensions measured in the comprehensive anthropometric survey of the lower limbs of US military personnel [Parham, et al. 1992]. A comparative analysis of the resulting data was performed to identify the pedal regions that evidence good conformance, and those that exhibit poor compliance, between the subjects' feet–ankles and the respective DLA DPSC footwear Lasts (and by extension the footwear manufactured from the Lasts that would be issued to the subjects under current military practice), Figures 11 and 12. Special attention was given to the measurements at the subjects' heels, as successfully fitting and functional footwear requires intimate compliance at the heel. Analysis of the data revealed a poor fit of the US Military Lasts at the heel for the majority of subjects sampled. Measurements of the subjects' heel width (W_{MalPDB}) at their medial malleoli posterior distal border [viz, at $(x, y)_{MalPDB} = (0.333*L_{HB}–0.05*L_{HB}\ ,\ 0.220*L_{HB})$], and in the same cross sectional plane at the level of maximum width (W_{Max}), normalized by each subject's respective foot heel-to-ball center length (L_{HB}), show approximate Gaussian distributions with sizable dispersions (mean $W_{MalPDB}/L_{HB} \pm\sigma = 0.3605$ mm/mm ±0.02785, and mean $W_{Max}/L_{HB} \pm \sigma = 0.4034$ mm/mm ±0.02290), Figure 13a. The differences in the distributions of W_{MalPDB} and W_{Max} reflect significant variations among the subjects' heel dimensions and contours (they evidence only mild correlation with a correlation coefficient of $R^2_{W_{MalPDB}-W_{Max}} = 0.6120$).

Similarly, the regression plot of the subjects' normalized heel width W_{MalPDB}/L_{HB} versus their normalized ball width W_{Ball}/L_{HB} shows a wide dispersion with weak to negligible correlation, $R^2_{W_{MalPDB}-W_{Ball}} = 0.2509$, Figure 13b. This further reflects the fact that individuals' foot–ankle shapes vary significantly and are **not** algebraically scaled. Similar results (though with a slightly larger heel width/heel-to-ball center length ratio) were observed for a sample of 25 VA NYHHS male veterans. This indicates that to properly accommodate and fit military personnel's feet, footwear should be manufactured and issued in several sizes of heel widths, for each respective heel-to-toe length and metatarsal ball width size. Doing so would significantly enhance footwear fit and functional performance, and undoubtedly reduce the incidence of foot and ankle trauma suffered by military personnel (particularly female personnel) during basic training and subsequent active duty.

Footwear Biomechanical Studies — Investigations measuring pedal/footwear interface stresses, ground reaction forces, and subject body segment kinematics during stance and gait, while wearing footwear with commonly prescribed orthopedic components and modifications, were performed. Tests were conducted with five subjects measuring pedal dorsal and plantar regional interface stresses, ground reaction forces, step and stride lengths, velocities and accelerations, and limb and body segment kinematics using Tekscan FScan and Flexiforce pedal stress transducers, a CIR Systems GaitRite Electronic Walkway, a Kistler force plate, and a Qualisys 3-D Video Motion Analysis System. Studies were performed to quantify the effects of three common orthopedic footwear components — scaphoid pads (arch supports), metatarsal pads, and heel pads. The effects of variations in pad thickness and longitudinal and latitudinal dimensions were investigated and categorized as a function of resulting interface stress and associated subject comfort rating, Figure 14. Study results showed that the pads affected loading in the regions of respective pad application, as well as in adjacent pedal regions. Although the differences in the stresses produced by the different pads often were not large, their affects on the subject's level of comfort changed abruptly. The resulting pedal sensitivity evidenced to small changes in loading, complicates pedorthic treatment, especially in individuals with peripheral neuropathy, such as those with chronic Diabetes Mellitus.

Studies were also performed on the effects of shoe outer sole wedges and heel wedges on pedal/footwear interface stress magnitudes, load spatial distribution, load temporal duration, and associated lower limb kinematics. The results of variations in sole and heel wedge thickness showed that 8mm sole and heel wedges can effectively reduce the loading on the respective side of the foot on which they are applied, Figure 15. Wedges of decreasing thickness were seen to evidence less effect, until at 2mm thickness their effect was found to be negligible. The effects of rocker soles on pedal plantar stress magnitudes, load spatial distribution, temporal load duration, and lower limb kinematics, were also studied as a function of rocker radius of curvature and fulcrum position. Study results showed that rocker soles, depending upon the location of the fulcrum and the angle of inclination of the rocker, can effectively unload the metatarsal heads and shorten the heel rise-to-toe off phase of the gait cycle, but doing so increases the loading incurred in the midfoot. Similarly, the effects of variation in shoe outer sole width were investigated. As shown in Figures 16 – 18, extended width soles and heels can be used to augment the stability of subjects with neuromuscular impairments, particularly diabetics suffering peripheral neuropathy. Increased sole–heel widths of ½ inch (¼ inch per side) were found to measurably augment the stability of neuropathic subjects, smoothing the trajectory of their center of mass, enabling a more normal, less strenuous, energy efficient gait (with a more normal percentage of single limb support vs. double limb support time over the gait cycle). Further increases in width above ½ inch, although helpful for

supplementation of mediolateral stability, were counter productive in some subjects with narrow base gaits, leading to striking of the contralateral heel during swing. Increases in width smaller than ¼ inch were found to afford minimal to immeasurable changes in stability.

In further biomechanical studies, the compressive creep response of the pedal plantar tissue at the heel and at the first metatarsal head of eight subjects' feet were measured using the VA NYHHS servo-optoelectromechanical tissue indentor [Houston, et al. 1998c], Figure 19. Magnetic resonance (MR) scans of two of the subjects' feet were also acquired, Figure 26, and the resulting MR images of their feet segmented with respect to tissue morphology and digitized. Corresponding nonlinear, finite element (FE) segmental models of the subjects' feet were developed at their heels and at their first metatarsal heads, from the MR images and respective tissue mechanical properties. The FE models constructed were used to analyze the stresses and strains incurred at the heel and at the metatarsal heads under normal loading conditions, and in the presence of a vertical calcaneal osteocyte (heel spur), as a function of pedorthic insole treatment with a range of material stiffnesses and design geometries, Figures 20 – 24, Tables 3 and 4. Results from these studies show maximum stresses and strains in pedal plantar tissues occur directly underneath the calcaneus and first metatarsal head, underneath and adjacent to the calcaneus and first metatarsal head. Alteration of insole material stiffness was shown to have little effect. Alteration of insole design geometry by introduction of reliefs, either removing material or by incorporation of softer secondary materials under the heel and metatarsal heads (as is common practice) was also shown to only minimally affect tissue stresses and strains. Incorporation of appropriate reliefs did, however, slightly reduce associated strain energy densities in the tissues. Because of the Dunnell effect, use of non-contoured, cylindrical reliefs introduced large localized stresses, strains, and stress gradients in pedal tissues at the border of the relief. Such design geometries should, therefore, be avoided. The greatest reductions in stress, strain, and strain energy magnitudes were achieved by custom contouring of insoles to match patients' "natural" pedal tissue geometry, and by proximally extending the insole borders around the fat pad to constrain its rheological displacement under load. Production of orthopedic insoles for personnel with this optimal design geometry out of a viscoelastic material three to four times the stiffness of the subject's pedal plantar tissues, was shown to enable reductions as high as 50% in maximum tissue stresses and strains, and 90% in maximum strain energy densities, during stance. In pathologic cases with calcaneal osteophytes (heel spurs) and/or arthritic osseous deformities with vertical components, reductions of as much as 95% in tissue stresses and strains, and 98% in strain energies densities were shown to be attainable in stance with custom contoured insoles that constrain soft pedal tissue displacement.

Footwear Material Mechanical Testing — Samples of the four materials most commonly used in manufacture of orthopedic insoles (i.e., polyurethane foam, polyethylene foam, silicone, and ethyl vinyl acetate foam (EVA)) were obtained. Specimens of each material in two different densities (Shore Hardness durometers) were prepared, and mechanical tests were performed in accordance with ASTM prescribed procedures, measuring the materials' respective mechanical stiffnesses in creep and stress relaxation under normal and shear loads, Figure 25. Measurement of the respective materials' load damping response, impact response, hysteresis, and plastic deformation (set) is continuing. Results from the material creep and stress relaxation response tests were used in the project FEA pedal plantar tissue biomechanical loading studies described in the previous section. Sample insoles of the respective materials were also prepared and tested under static, axially applied loads (approximately $\frac{1}{4}^{th}$ body weight) with one experimental subject in the VA NYHHS magnetic resonance scanner, Figures 26 and 27. The MRI scan results were used to compute the values of pedal tissue strain incurred during static, axial loading as a

function of pedorthic insole stiffness and geometric design. These computations are, in turn, being used to validate and refine the project pedal FE models.

To improve pedorthic treatment for subjects suffering metatarsalgia, plantar fasciitis, heel spurs, and/or chronic Diabetes with Charcot conditions of their feet and ankles, additional footwear design studies were conducted. Initial designs for footwear outer soles incorporating cushions under the heel, the metatarsal heads, and/or the midfoot were developed, Figure 28. As seen in Figure 26, the designs formulated mimic the anatomical structure of the pedal plantar fat pad, incorporating sealed, "honey comb" like septae, which function like miniature fluid damping cylinders to dissipate and disperse locally applied loads. Molds were made from the respective cushion CAD design drawings, and initial prototype cushions were fabricated in a range of durometers. In addition, 3-D, sectional FE models of the cushions were generated to study the effects of cushion material stiffness, septal wall thickness, and septal cylinder internal fluid media, on load damping and dispersion performance. This work is continuing.

Key Research Accomplishments

- Specifications were developed, components procured, and a prototype 3-D Pedorthic Optical Digitizer assembled, calibrated, and laboratory and clinically tested.
- The software required for: (i) control of the digitizer; (ii) measurement acquisition, processing, analysis, visualization, and registration; and (iii) for post-processing of digitizer measurements for automatic detection, identification, and registration of pedal fiduciary anatomical landmarks, was created and tested.
- 144 US military footwear Lasts were digitized with the optical digitizer, and the resulting measurement files entered into the VA NYHHS Pedorthic CAD System Last Library, and into the project pedorthic database
- Optical scans and manual measurements of the feet and ankles of 43 normal, healthy female test subjects of military service age, were acquired and used in quantitative assessment of military footwear/Last fit. Analysis of the scans and measurements showed that military Lasts/footwear properly fit only one third of the subjects sampled. A metric(s) for heel width, therefore, needs to be used, in addition to heel-to-toe length and metatarsal ball width to manufacture and issue footwear, and assess footwear fit to military personnel.
- The compressive creep response of eight subjects' pedal plantar tissues was measured. Magnetic resonance (MR) scans of two of the subjects' feet were acquired and digitized, and the results used to create sectional finite element models of their feet at the heel and at the first metatarsal head. The FE models developed were used in studies to optimize pedorthic insole design for prevention and treatment of podalgia, metatarsalgia, plantar fasciitis, and calcaneal osteocytes. The resulting FE model calculations of pedal plantar tissue stresses and strains, together with MR scan measurement of actual tissue strains, show only insoles custom contoured to match individuals' pedal morphological shapes, and which limit pedal soft tissue displacement, effectively reduce tissue stresses and strains. The project FEA study results further provide convincing evidence that non-recovered (inelastic) strain energy dissipated in pedal tissues, is responsible for chronic, repetitive loading injuries, and not applied stresses, as commonly supposed. Measured levels of pedal tissue plantar and dorsal stress deemed comfortable versus uncomfortable by test subjects show a very fine level of demarcation, which complicates pedorthic treatment, and further indicates tissue strain plays

a bigger role than stress in limiting comfort/discomfort and trauma at load magnitudes below critical yield and failure levels.

- In biomechanical studies, measurements were acquired for analysis and quantification of the effects of three orthopedic components – scaphoid pads, metatarsal pads, and heel pads – on (i) pedal/footwear interface stress magnitudes, gradients, temporal duration, and spatial distribution; (ii) on ground reaction force magnitudes, locations and durations; and (iii) on lower limb kinematics. Similarly, the effects of shoe outer sole and heel wedges; rocker sole radius of curvature and fulcrum position; and of shoe outer sole and heel width, on pedal/footwear interface stresses, ground reaction forces, and limb kinematics were investigated. Results showed that orthopedic footwear components and modifications can and do affect loading in their regions of application, as well as in adjacent pedal regions. Furthermore, the differences in the stresses produced by parametric variations in the respective orthopedic components/modifications typically are not large, but their corresponding effects on subjects' level of comfort/stability frequently changes significantly.
- The creep response and stress relaxation response (characterizing the mechanical stiffness) of four of the most commonly used pedorthic insole materials were measured; magnetic resonance scans of the feet of two test subjects statically, axially loaded wearing insoles, fabricated from the respective materials in a range of design geometries, were acquired. Measurement of tissue strains from the MR scans, together with results from the project FEA analyses show that reductions in pedal tissue stresses, strains, and strain energies afforded by pedorthic insole materials with different durometers and elasticities are small. The greatest reductions in stress, strain, and strain energy are obtained by custom contouring insoles to match subjects' "natural" pedal tissue contours and by extending the insole borders proximally around the pedal fat pad to constrain its rheological displacement under load. Production of orthopedic insoles for personnel with this optimal design geometry out of a viscoelastic material three to four times the stiffness of the subject's pedal plantar tissues, enables reductions as high as 50% in maximum tissue stresses and strains, and 90% in maximum strain energy densities, to be achieved. In pathologic cases with calcaneal osteophytes (heel spurs) and/or arthritic osseous deformities, reductions of as much as 95% in tissue stresses and strains, and 98% in strain energies densities can be attained with optimally designed insoles matched to the individual's pedal morphological contours.

Reportable Outcomes

Manuscripts & Abstracts

- Houston VL, Luo G, Mason CP, Mussman M, Garbarini MA, Beattie AC, Cruise CM, Thongpop C. "FEA Optimization of Pedorthic Insole Design for Patients with Diabetes Mellitus." **Proc. 10th World Congress ISPO**, Glasgow, UK, July 2001; Tho10.7.
- Houston VL, Luo G, Mason CP, Mussman M, Garbarini MA, Beattie AC, Cruise CM, Thongpop C. "FEA Optimization Of Pedorthic Treatment For Podalgia," **ASME Advances in Bioengineering**, 2001; BED-Vol. 51.
- Houston VL, Luo GM, Mason CP, Beattie AC, Garbarini MA, Thongpop C. "Optimization of Pedorthic Insole Design." **Proc. 3rd Annual VA Rehabil Res & Devel Conf**, Arlington, VA, Feb 2002.

Presentations

- Houston VL, Luo G, Mason CP, Mussman M, Garbarini MA, Beattie AC, Cruise CM, Thongpop C. "FEA Optimization of Pedorthic Insole Design for Patients with Diabetes Mellitus." **Proc. 10th World Congress ISPO**, Glasgow, UK, July 2001.
- Houston VL. "Optimization Of Pedorthic Insole Designs". 2001 Annual Mtg Texas Orthotics and Prosthetics Association, Brownsville, TX, September 28, 2001.
- Houston VL. "Pedorthics Fitting & Functional Assessment." Department of Veterans Affairs Research Day, April 8, 2002, VA NYHHS, Brooklyn, NY
- Houston VL. "Tissue Biomechanical Modeling & Loading Analysis." Department of Veterans Affairs Research Day, April 8, 2002, VA NYHHS, Brooklyn, NY

Informatics

- Pedal 3-D Geometric Database established with optical scans and fiduciary manual measurements of the feet/ankles of 43 subjects of military service age.
- Optically digitized measurements of 144 US military footwear Lasts were added to the Last Library of the VA Pedorthic CAD/CAM System, and to the project pedorthic database.

Conclusions

Specifications were created, and components procured and assembled for a pedorthic optical digitizer. The prototype digitizer was calibrated, and laboratory and clinically tested. The software required for control of the digitizer, and for digitizer camera measurement acquisition, processing, visualization, and analysis, with automated detection, identification, and registration of fiduciary anatomical landmarks, was created and tested. 144 DLA DSPC Lasts for US military footwear were digitized, and the resulting measurement files entered into the VA NYHHS Pedorthic CAD System Last Library. The feet–ankles of 43 normal, healthy female subjects of military service age were optically scanned and measured. The resulting measurements were then analyzed and used in quantitative assessment of military footwear/Last fit. Analysis showed that military footwear/Lasts properly fit only one third of the subjects sampled. Thus, a metric for heel width needs to be established and used, in addition to heel-to-toe length and metatarsal ball width, to manufacture, issue, and assess the fit of footwear for US military personnel. Instrumentation was calibrated and tested for measurement of pedal/footwear interface stresses, ground reaction forces, and body segment kinematics for quantification of footwear fit and function. Biomechanical studies of orthopedic footwear modifications and component designs were performed, measuring the effects of variations in design of three common orthopedic footwear components – scaphoid pads, metatarsal pads, heel pads – as well measurement of the effects of shoe outer sole and heel wedges, shoe outer sole rocker curvature and fulcrum position, and increased outer sole and heel widths, on pedal/footwear interface stresses, ground reaction forces, and body segment gait kinematics. The nonlinear mechanical stiffness characteristics of pedal plantar tissue at the heel and at the first metatarsal head, together with the external and internal geometry and morphology of the feet and ankles of eight subjects were measured, and segmental finite element models of two of the subjects' feet were created. The mechanical properties of four of the materials most commonly used in production of pedorthic insoles were measured, and the results used, together with the pedal finite element models, in pedorthic insole design optimization studies for treatment and prevention of podalgia, metatarsalgia, plantar fasciitis, and calcaneal osteophytes. In addition, an initial design for

cushions to be incorporated in the outer soles of orthopedic shoes under the metatarsal heads, the heel, and the midfoot were developed, and prototypes in a range of durometers were fabricated for use in augmented treatment of subjects with these disorders.

The pedorthic optical digitizer developed in the project has been shown to provide accurate, repeatable and consistent measurements of the 3-D spatial geometry and surface topography of peoples' feet and ankles, in natural and prescribed orthopedic alignments, in partial and full weight bearing states, registering the spatial location of fiduciary anatomical landmarks. As such, the digitizer is a powerful tool. It can have numerous applications in Pedorthics, Podiatrics, and Orthopaedics. It can be employed at military induction and training sites to provide rapid and accurate measurements of inductees' feet–ankles for issuance of properly fitting and functional footwear, especially for female personnel, whose pedal morphology makes them more susceptible to injury in improperly fitting footwear. In addition, as demonstrated in field trials of the VA Pedorthic CAD/CAM System, the optical digitizer is an essential component for rapid acquisition and input of precise, comprehensive pedal measurements required for custom design and manufacture of well-fitting, comfortable and functional orthopedic footwear. In addition, in medical and podiatric applications, the digitizer is a powerful quantitative tool, useful in diagnosing and monitoring treatment of pathologies and disorders that affect pedal geometry, such as vascular insufficiency; edema; tissue inflammatory response to osseous degeneration from arthritis or Charcot syndrome; musculoskeletal deformity resulting from trauma or chronic systemic diseases such as diabetes or arthritis. The digitizer can also be used in anthropometric surveys, compiling measurements of the pedal geometry of a statistically significant and powerful sample of persons of military service age, for use in design of new, more anatomically compliant Lasts, that will permit production of better fitting, more functional, and more comfortable footwear.

Clinical use of the digitizer, providing rapid, accurate measurement of pedal geometry, coupled with knowledge acquired from biomechanical studies of pedal tissue mechanical characteristics, and pedorthic material properties, can lead to development of new, more accurate and comprehensive metrics of footwear fit, that will contribute to increased mobility and performance, and aid in prevention of pedal trauma in military personnel, veterans, and civilian pedorthics patients. Quantitative characterization of pedal tissue and pedorthic material mechanical properties, together with characterization of the pedal/footwear interface stresses, ground reaction forces, and limb segment kinematics during stance and gait, can lead to development of new pedorthic materials and creative designs that provide better fitting, more comfortable, and more functional footwear. As evident in the project pedorthic insole design studies summarized in Table 3, pedal tissue stresses and strains incurred under normal walking and standing conditions, are not exceptionally large. Nonetheless, some people suffer podalgia, metatarsalgia, plantar fasciitis, and/or heel spurs from repetitive activities. Their respective stress and strain magnitudes imposed on their pedal tissues do not change, only the loading duration is increased. The only parameter that differs appreciably in these cases is tissue strain energy density. Strain energies dissipated in pedal tissues from non-elastic deformation, can, and undoubtedly do, disrupt tissue circulation and metabolism, leading to pain and inflammation, which in turn can result in tissue structural changes and eventual mechanical failure. Development of new pedorthic insole and outer sole materials designed specifically to dissipate strain energies can alleviate this problem. New results, such as this, arising from quantitative, biomechanical studies, have the potential to significantly improve the function, comfort, and performance of footwear for military personnel, as well as that for veterans and civilians with podiatric and orthopedic pedal disorders and pathologies.

References

Boulton AJM. "Lowering the risk of neuropathy, foot ulcers, and amputations." **Diabetic Medicine**, 1998; 15 (Sup 4); S57–59.

Boulton AJM, Veves A, and Young MJ, "Etiopathogenesis and Management of Abnormal Foot Pressures," in **The Diabetic Foot,** 5th ed., Levin ME, O'Neal LW, and Bowker JH, eds., C. V. Mosby, St. Louis, MO, 1993; 234–246.

Coleman WC. "Footwear In a Management Program of Injury Prevention," in **The Diabetic Foot**, 5th ed., Levin ME, O'Neal LW, and Bowker JH, eds., C. V. Mosby, St. Louis, MO, 1993; 293–309.

D'Ambrosia RD. "Conservative Management of Metatarsal and Heel Pain in the Adult Foot," **Orthopedics**, 1987; 10: 137–142.

Donaghue VM, Sarnow MR, Giurini JM, Chrzan JS, Habershaw GM, and Veves A. "Longitudinal in-shoe foot pressure relief achieved by specially designed footwear in high risk diabetic patients," **Diabetes Res Clin Pract**, 1996; 31(1-3): 109–114.

Gould JS, "Conservative Management of the Hypersensitive Foot in Rheumatoid Arthritis," **Foot & Ankle**, 1982; 2: 224–229.

Houston VL, Mason CP, Beattie AC, LaBlanc KP, Luo G, Garbarini MA, and Cruise CM, "The VA-Cyberware Prosthetics-Orthotics-Pedorthics Optical Digitizers," in **CAD/CAM Systems in Pedorthics, Prosthetics & Orthotics**, U. Boenick and E.h.M. Nader, eds., Verlag Orthopadie-Technik, Berlin, Germany, 1998a; 133–163.

Houston VL, Mason CP, Luo G, Mussman M, LaBlanc KP, Beattie AC, Garbarini MA, and Cruise C. M. "An Overview of the VA Pedorthic CAD/CAM System," in **CAD/CAM Systems in Pedorthics, Prosthetics & Orthotics**, U. Boenick and E.h.M. Nader, eds., Verlag Orthopadie-Technik, Berlin, Germany, 1998b; 337–348.

Houston VL, Luo G, Mason CP, Arena L, Beattie AC, LaBlanc KP, Garbarini MA. "FEA for Quantification of Prosthetic/Orthotic/Pedorthic CAD," **CAD/CAM Systems in Pedorthics, Prosthetics & Orthotics**, U. Boenick and E.h.M. Nader, eds., Verlag Orthopadie-Technik, Berlin, Germany, 1998c; 254–276.

Houston VL, Mason CP, Beattie AC, LaBlanc KP, Garbarini MA, Lorenze EJ, and Thongpop CM. "The VA–Cyberware Optical Laser Digitizer," **J. Rehab. Res. & Devel.**, 1995 (February); 32(1): 55–73.

Janisse DJ. "Prescription footwear for arthritis of the foot and ankle," **Clin Orthop**, 1998; 349:100–107.

Janisse, DJ. "Pedorthic Care of the Diabetic Foot," in **The Diabetic Foot,** 5th ed., Levin ME, O'Neal LW, and Bowker JH, eds., C. V. Mosby, St. Louis, MO, 1993; 549–576.

Kelly VE, Mueller MJ, Sinacore DR. "Timing of peak plantar pressure during stance phase of walking." **J Amer Podiatric Med Assoc**, 2000 (Jan); 90 (1): 18–23.

Lord M, and Hosein R. "Pressure Redistribution By Moulded Inserts," **Proc. 7th World Congress ISPO, Chicago, IL, June 1992**; 279.

Moncur C, and Shields MN. "Clinical Management of Metatarsalgia in the Patient With Arthritis," **Clinical Management in Physical Therapy**, 1983; 3(4): 7–13.

Mueller MJ. "Application of plantar pressure assessment in footwear and insert design." **J Orthopaedic & Sports Physical Therapy**, 1999 (Dec); 29 (12): 747–755.

Mueller MJ, Sinacore DR, Hoogstrate S, and Daly L. "Hip and Ankle Walking Stratagies: Effect on Peak Plantar Pressures and Implications for Neuropathic Ulceration," **Arch Phys Med Rehabil**, 1994; 75: 1196–1200.

Parham KR, Gordon CC, Bensel CK. "Anthropometry of the Foot & Lower Leg of US Army Soldiers," US Army Natick Res, Devel, Engr Cntr Tech Rpt. TR–92/028, Natick, MA 1992.

Reinker KA, Ozbourne S. "A Comparison of Male and Female Orthopedic Pathology In Basic Training," **Military Med.**, 1979; 144: 532–536.

Riddle DL, and Freeman DB. "Management of a Patient With Diagnosis of Bilateral Plantar Fasciitis and Achilles Tendonitis," **Physical Therapy**, 1988; 68(12): 1913–1916.

Rodgers MM, and Cavanagh PR. "Pressure Distribution in Morton's Foot Structure," **Med. & Sci. in Sports & Exercise**, 1989; 21(1): 23–28.

Rose NE, Feiwell LA, and Cracchiolo A. "A Method for Measuring Foot Pressures Using a High Resolution, Computerized Insole Sensor: The Effect of Heel Wedges on Plantar Pressure Distribution and Center of Force," **Foot & Ankle**, 1992; 13(5): 263–271.

Ross J, Woodward A. "Risk Factors For Injury During Basic Military Training," **J. Occup. Med.**, 1994; 36: 1120–1126.

Schaff PS. "An Overview of Foot Pressure Measurement Systems," **Clin Podiatric Med Surg**, 1993; 10(3): 403–415.

Schaff PS, and Cavanagh PR. "Shoes for the Insensitive Foot: the Effect of a 'Rocker Bottom' Shoe Modification on Plantar Pressure Distribution," **Foot & Ankle**, 1990; 11(3): 129–140.

Tovey FI, and Moss MJ. "Specialist Shoes for the Diabetic Foot," in **The Foot in Diabetes**, Connor H, Boulton AJM, and Ward JD, eds., Wiley & Sons, New York, NY, 1987; 97–108.

van Schie C, Ulbrecht JS, Becker MB, Cavanagh PR. "Design criteria for rigid rocker shoes." **Foot Ankle Intl.**, 2000 (Oct); 21 (10): 833–844.

Wosk J, and Voloshin AS. "Low Back Pain: Conservative Treatment With Artificial Shock Absorbers," **Arch. Phys. Med. & Rehabil.**, 1985; 66: 145–148.

Wunderlich RE, Cavanagh PR. "Gender Differences in Adult Foot Shape: Implications for Shoe Design." **Med Sci Sports Exerc**, 2001; 33(4): 605–611.

Young CR. "The FScan System of Foot Pressure Analysis." **Clin Podiatric Med Surg**, 1993; 10(3): 455–461.

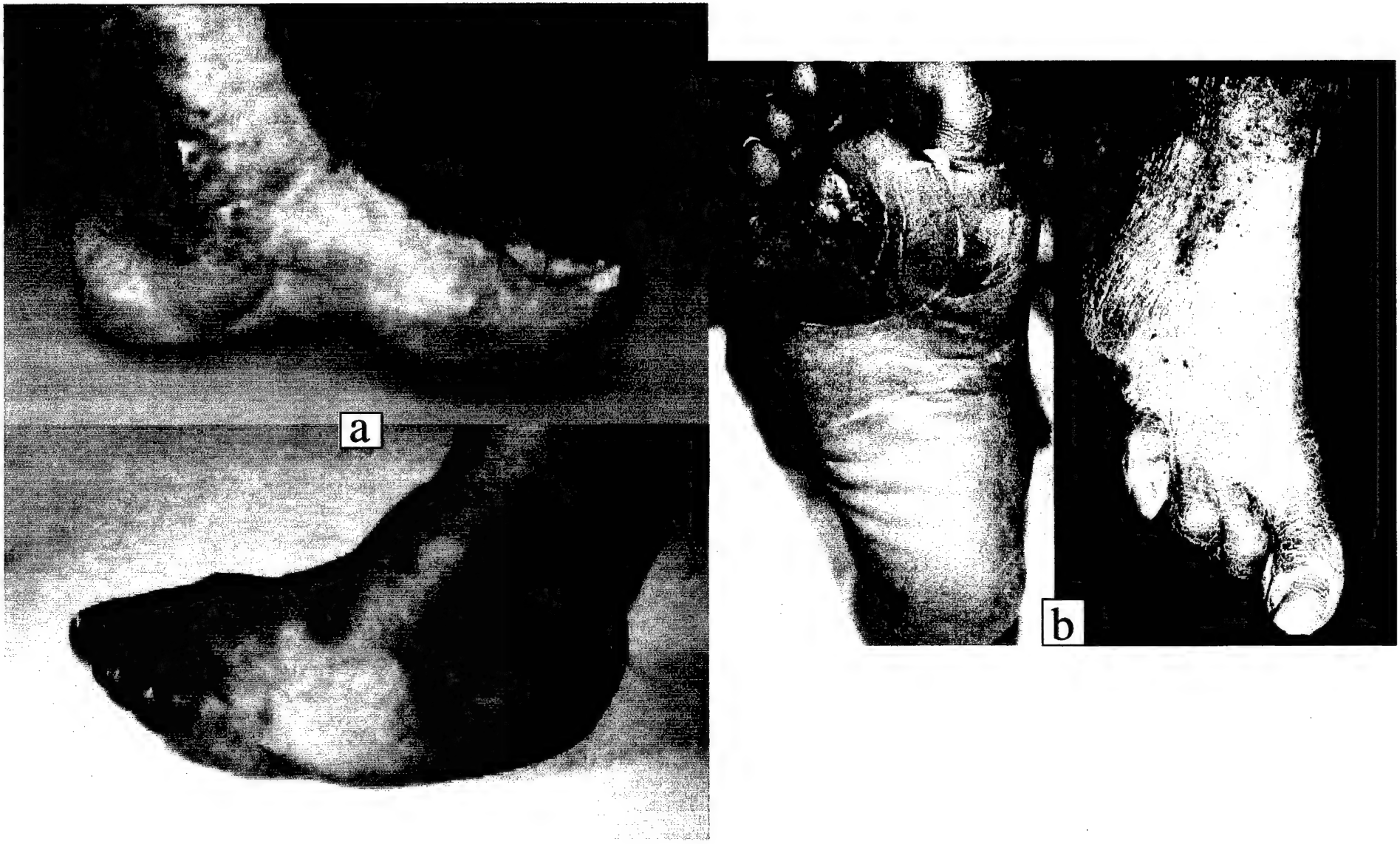

Figure 1. The feet–ankles of US Veterans requiring custom orthopedic footwear. (a) (top) Veteran with pedal injury from shrapnel with consequent fused mid-foot; (bottom) paratrooper with impact injury to mid-foot; (b) Veterans with chronic Diabetic Mellitus with — (left) stage 3 decubitus ulcer under third metatarsal head; (right) resected fifth ray of forefoot from repetitive stress injury and consequent tissue necrosis and gangrene.

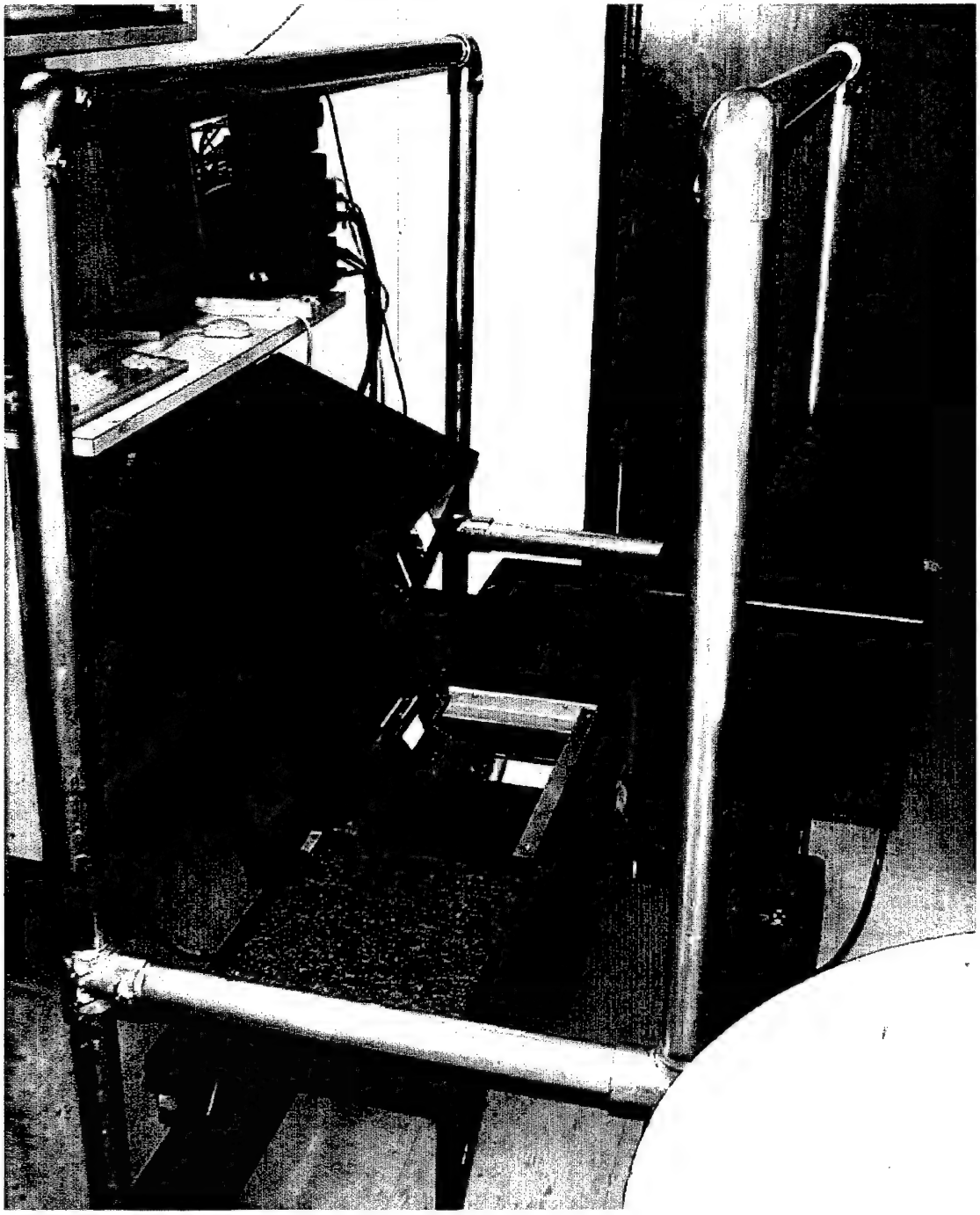

Figure 2. VA NYHHS Pedorthic Optical Digitizer.

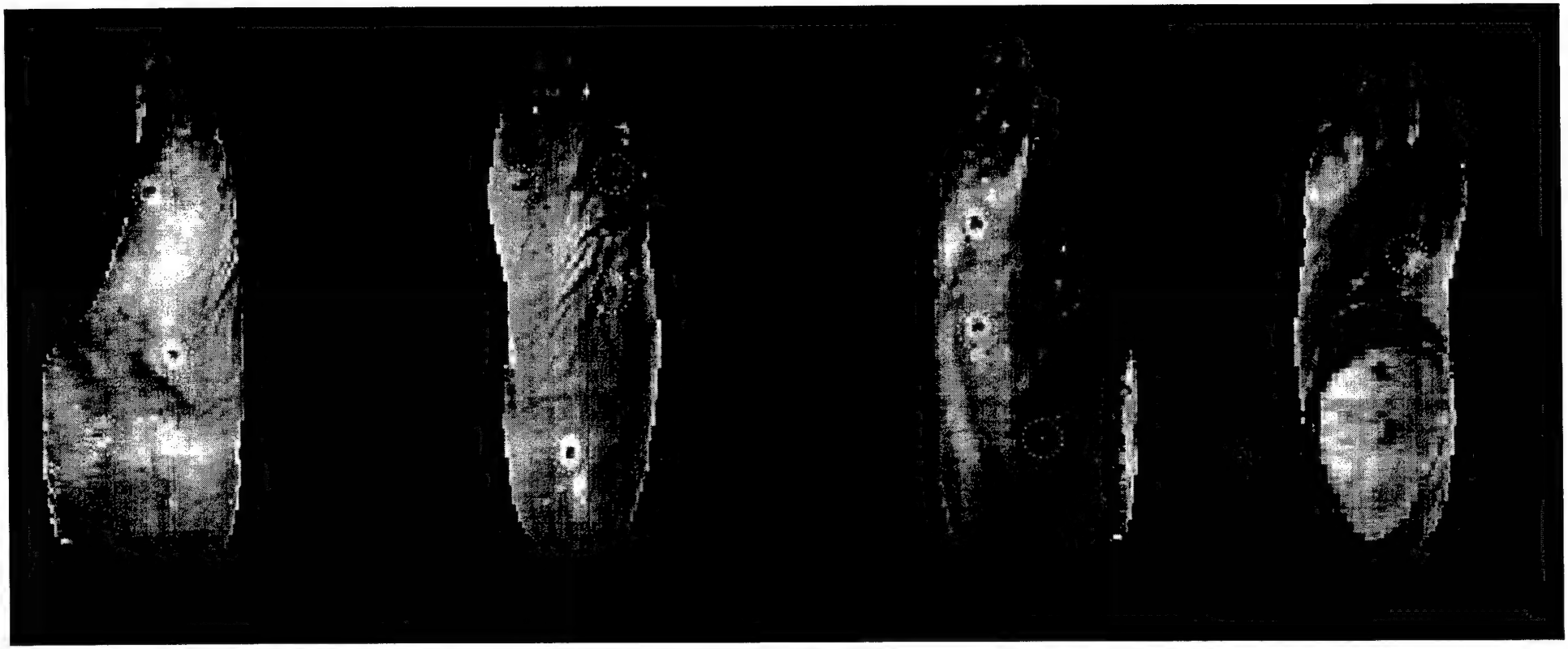

Figure 3a. Images of the scan of a test subject's foot-ankle with the VA NYHHS Pedorthic Optical Digitizer after post-processing camera output intensity and range data with the automatic landmark detection, identification, and registration (ALDIR) algorithm. Differences in the intensity of the laser signal reflected from the pedal surface and from the fiduciary landmarks are evident in the scan data. The encircled points are the landmarks detected by the ALDIR neural network algorithm.

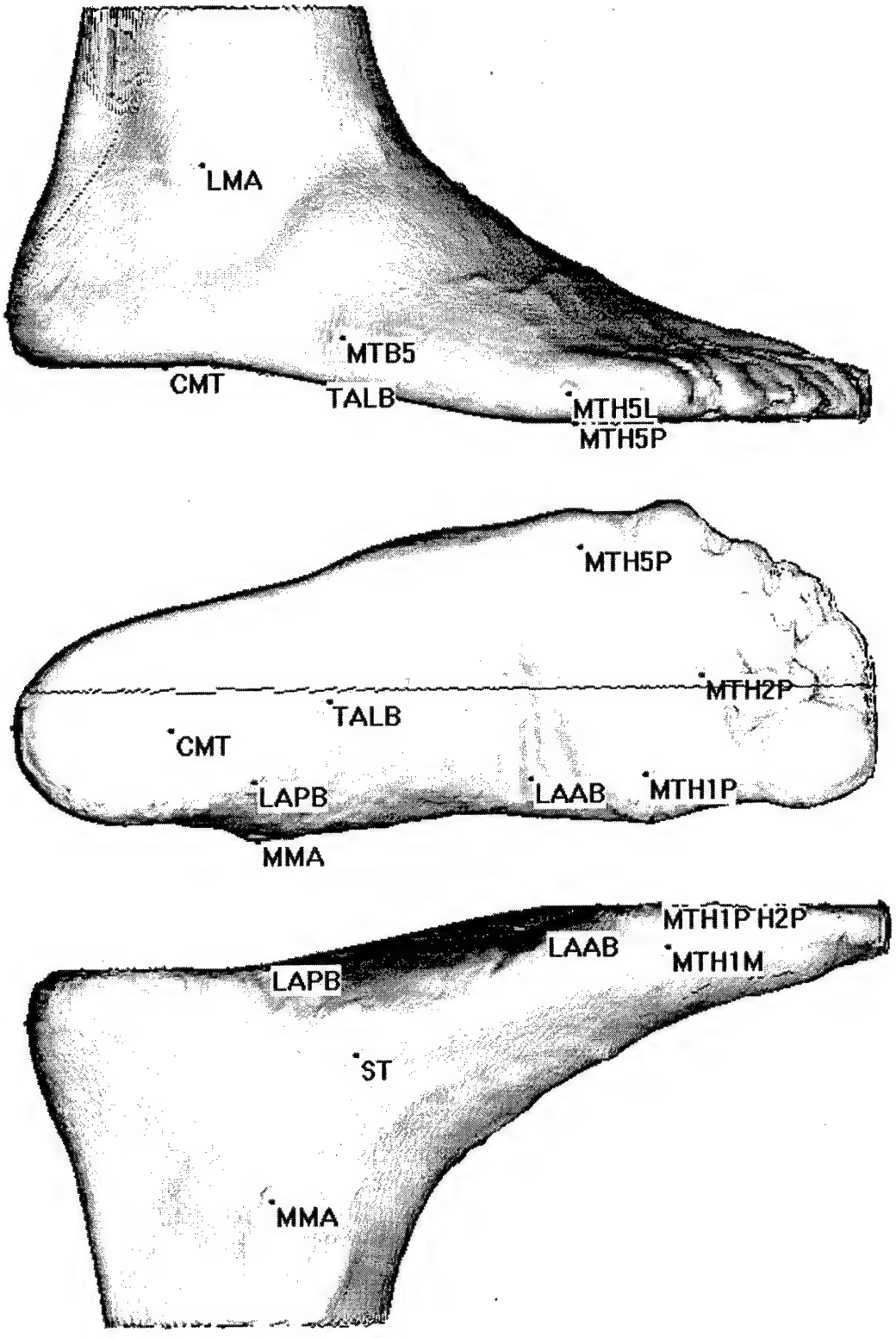

Figure 3b. Principal orthogonal views of the shaded solid image of a test subject's foot-ankle, shown after post-processing the optical scan measurements with the VA NYHHS (ALDIR) algorithm and import of the resulting data int the VA NYHHS Pedorthic CAD.CAM System for custom orthopedic footwear design and manufacture.

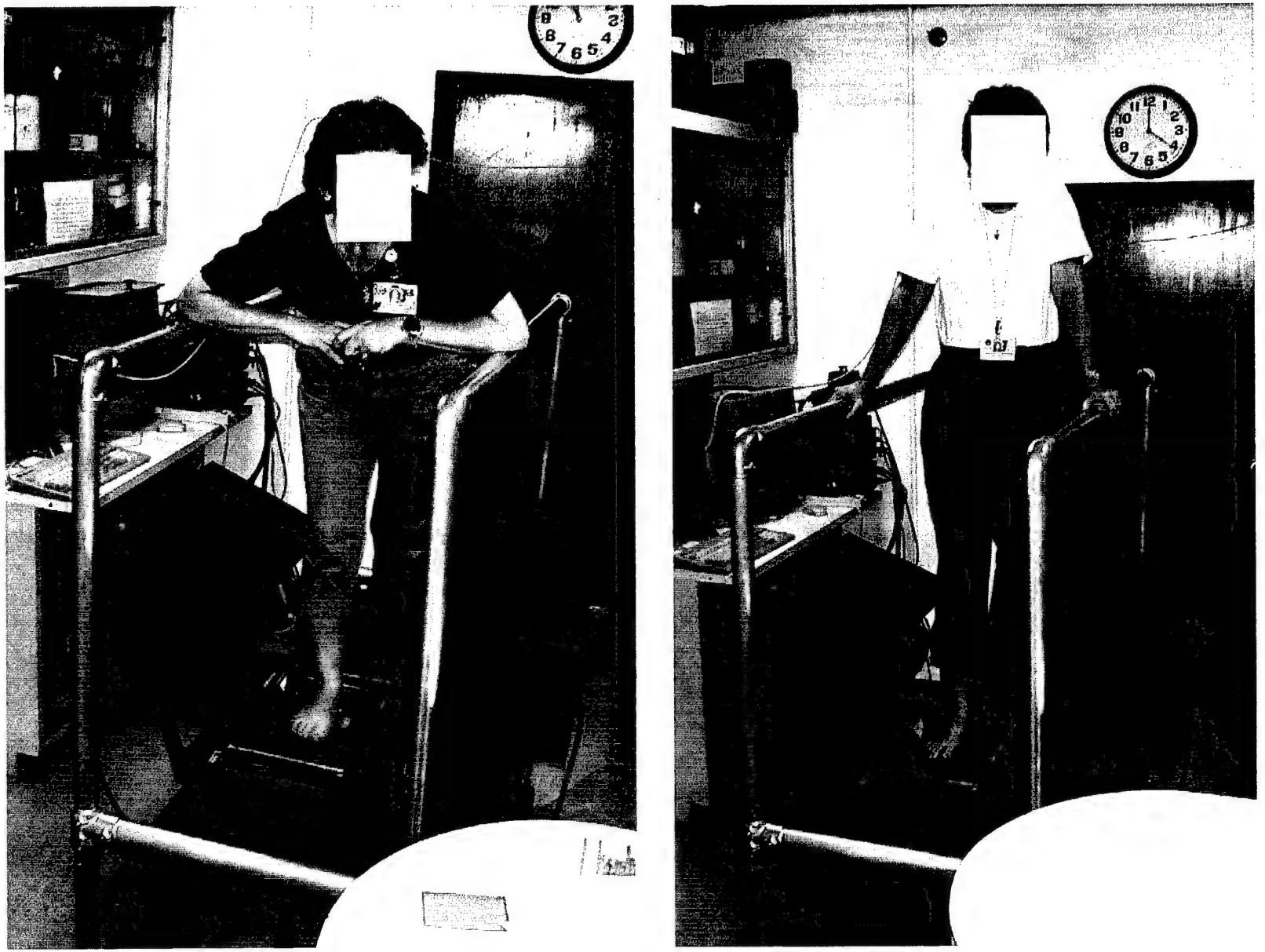

Figure 4. Digitization of the feet-ankles of two VA NYHHS Rehabilitation Engineering Research test subjects in the Pedorthic Optical Digitizer.

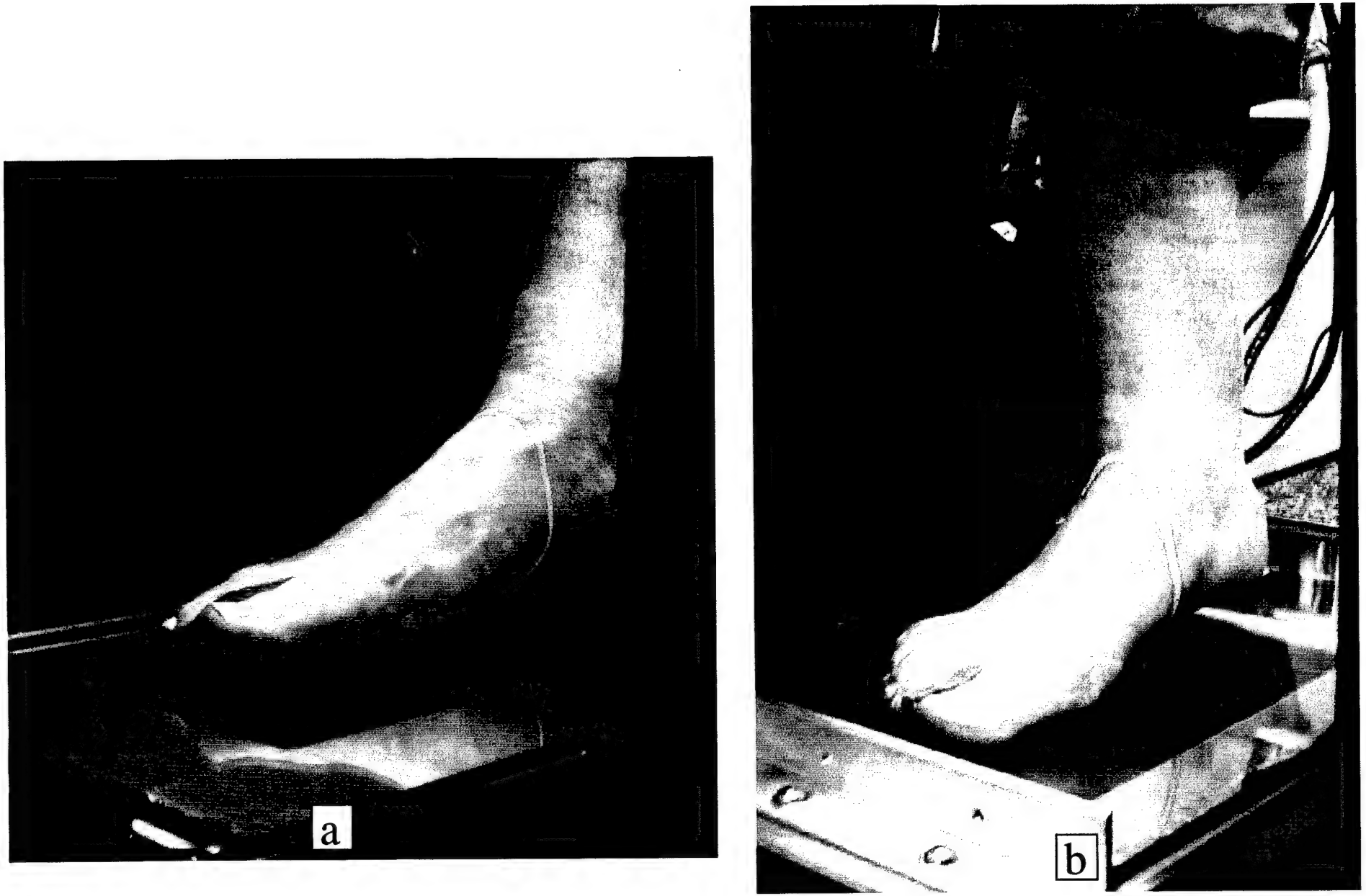

Figure 5. Optical scans of a test subject's foot-ankle on: (a) a flat, transparent, support platen and (b) on an orthopedically contoured platen. Refractive distortion and multiple, spurious reflections of the composite intra- and inter- scan head laser signals are evident especially for the scan with the contoured platen.

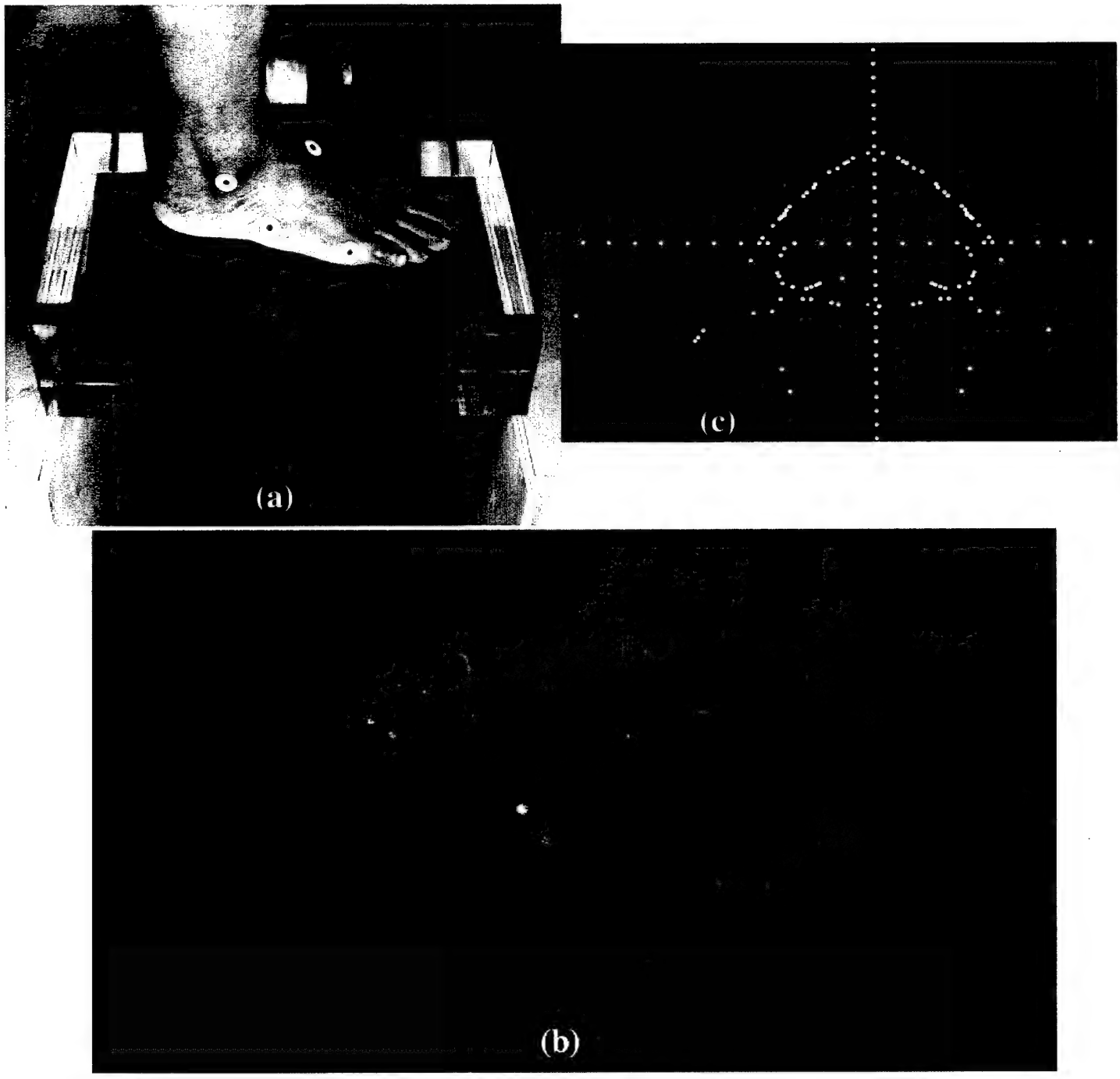

Figure 6. **(a)** Laboratory testing, measuring the transmissivity and refractivity of the orthopedically contoured pedal support platen, fabricated from transparent, low refractive index Lucite™. The incident near infrared source signal and multiply reflected constituent secondary and tertiary signals are visible. **(b)** Demonstration showing multiply reflected and refracted "noise" constituents (small red dots) of an incident source signal (large red dot); **(c)** Transverse cross section through the forefoot from a pedal scan illustrating corruption of the digitizer camera output signal from multiply reflected and refracted signal constituents.

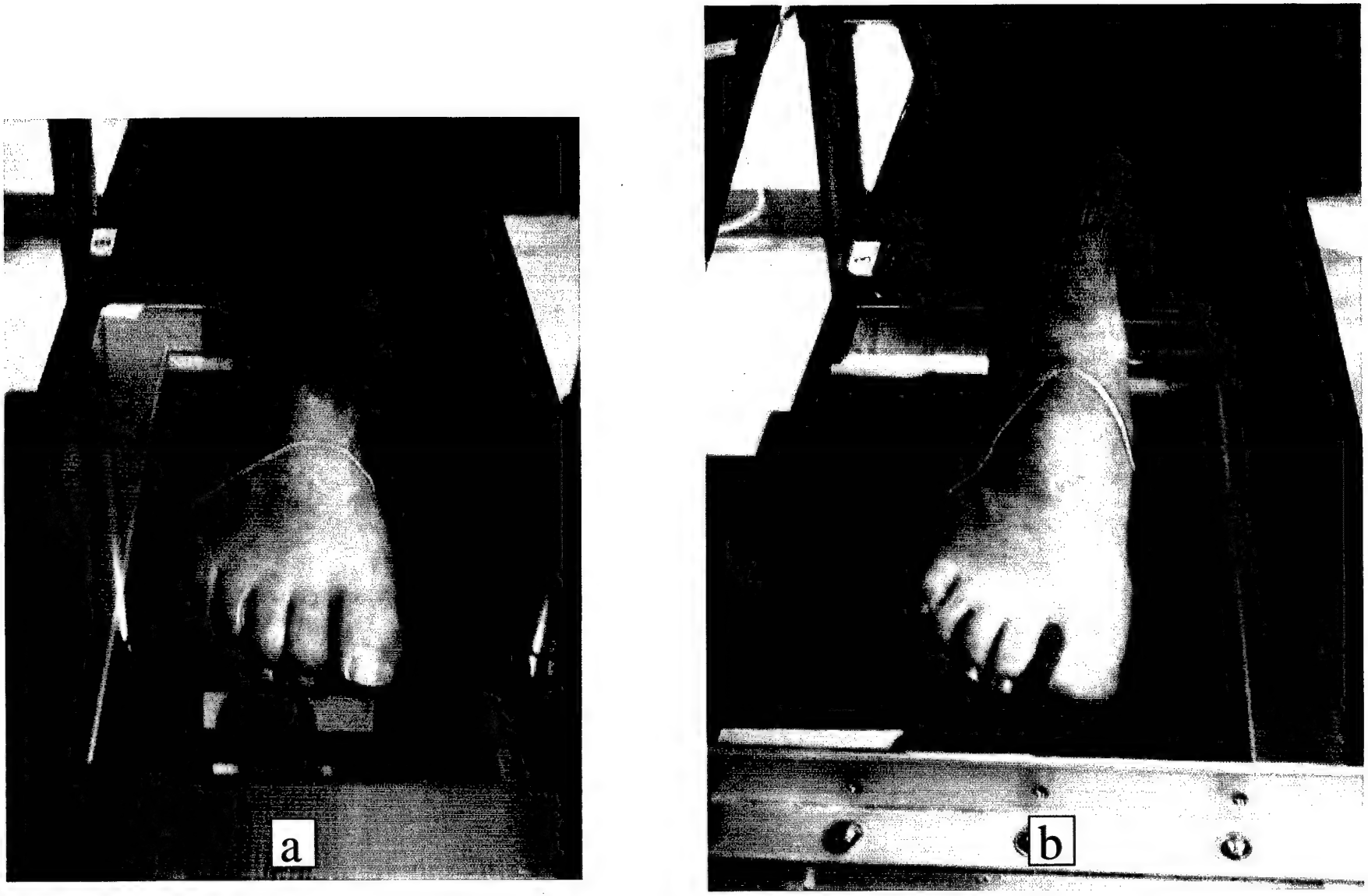

Figure 7. Optical scans of the foot-ankle of a test subject on the orthopedically contoured platen: (a) without, and (b) with a matching contoured, black (optically opaque) silhouette placed along the lateral border of the subject's foot to minimize corruption of the camera images from spurious, multiple reflections of the incident laser signals.

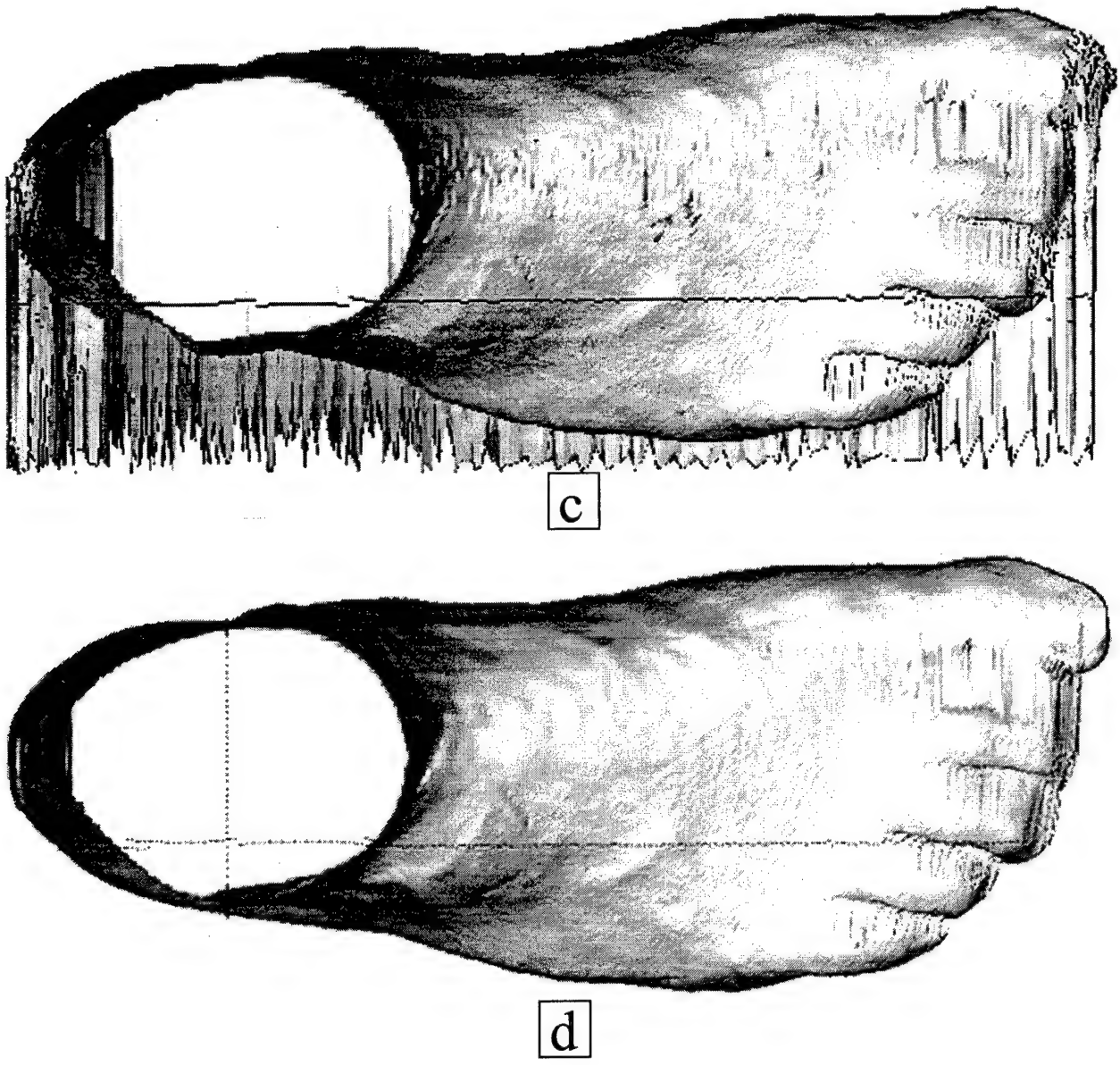

Figure 7 (*cont.*) Shaded solid images of the resulting optical scan measurements: (c) acquired without a black opaque border; and (d) with a contoured opaque border. The corruption of the resulting scan measurements from multiple reflections is clearly visible in (c).

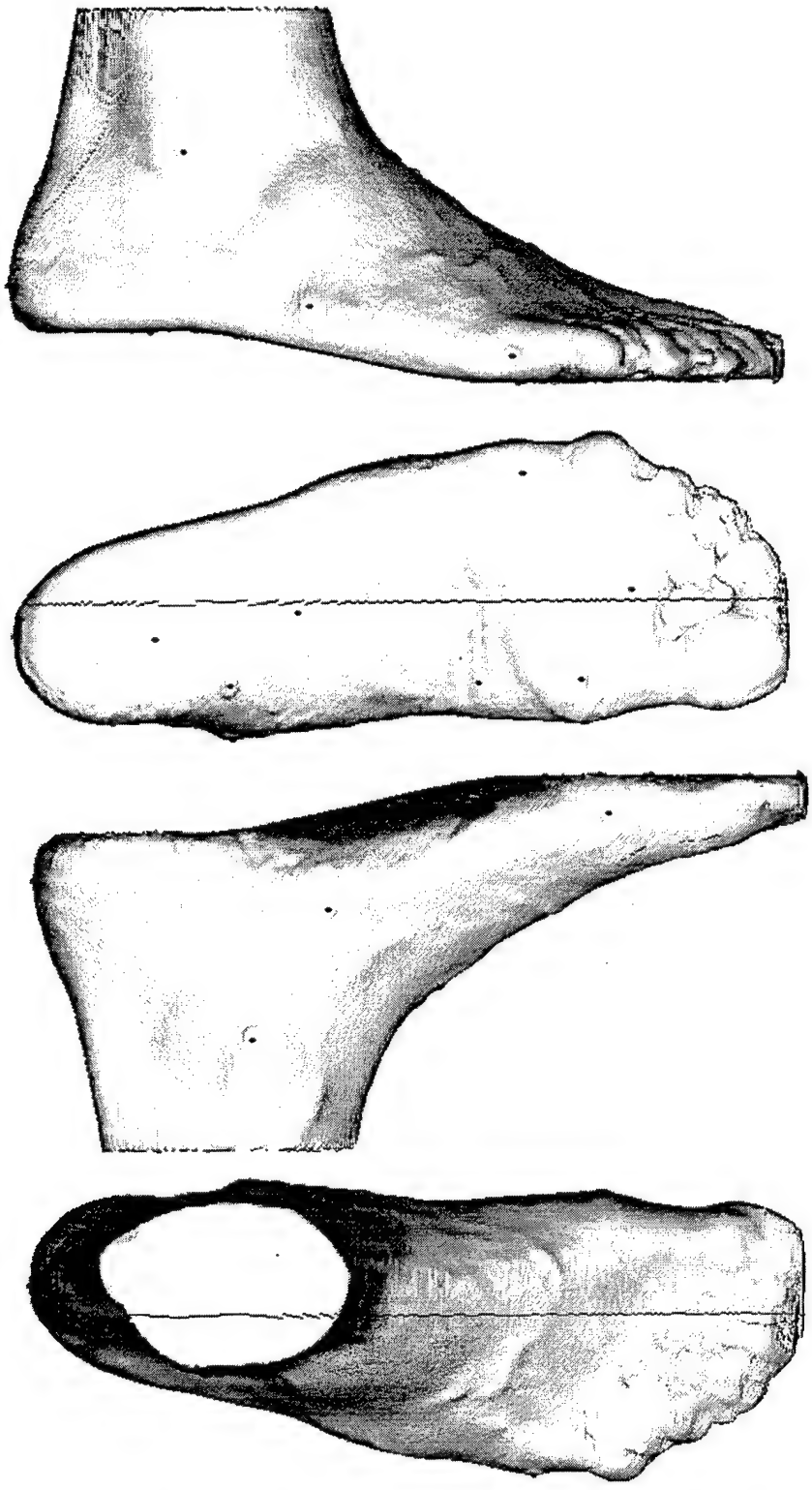

Figure 8. Four principal orthogonal views of the optical scan of a test subject's foot-ankle displayed in the VA NYHHS Pedorthic CAD/CAM System. Scan measurements were acquired with the VA NYHHS Pedorthic Optical Digitizer employing the "workarounds" developed to mitigate signal distortion and corruption from refractory effects and spurious noise from multiple reflections. In addition, Play-Doh filler has been inserted between the subject's toes to prevent multiple segmentation of the phalangeal data, and thus allow representation of the scan data in cylindrical coordinates.

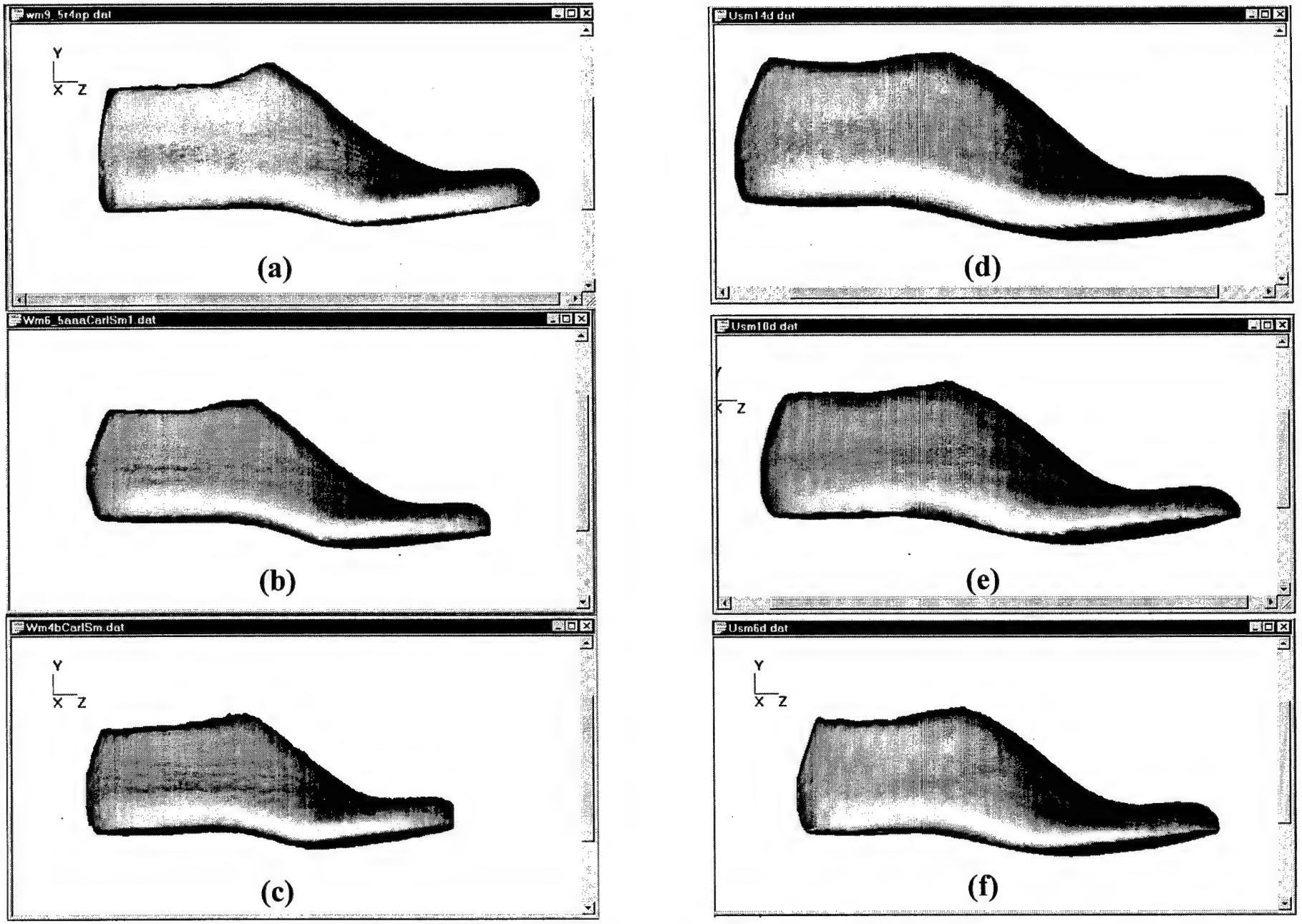

Figure 9. Shaded solid sagittal views of the DLA DPSC US Military Lasts for female personnel (a – c) and for male personnel (d – f) displayed in the VA Pedorthic CAD System. Digitized scans of the smallest, mid-size, and largest Lasts in the respective sets are shown. The algebraic (non-anatomical) scaling of the Lasts is evident.

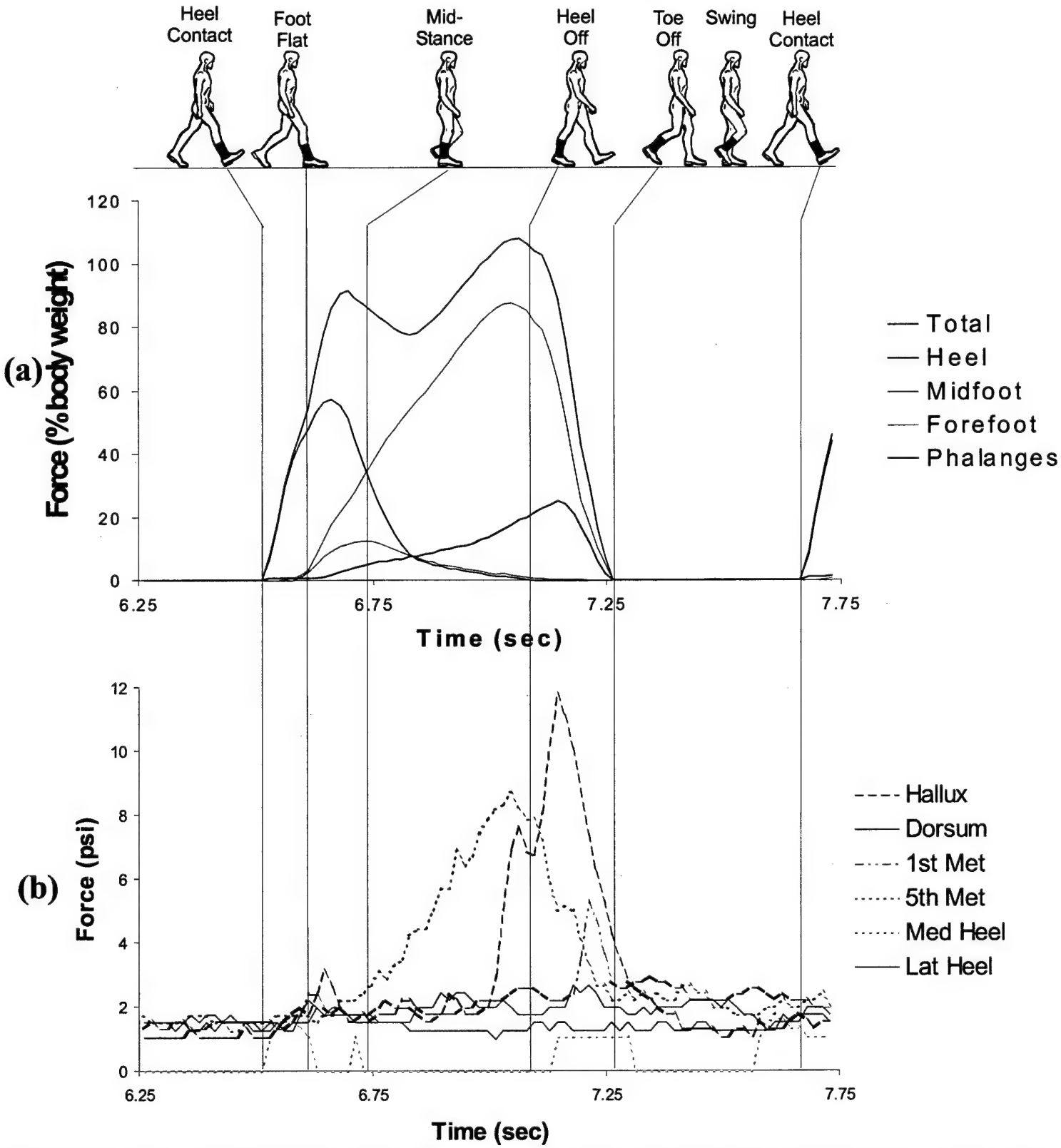

Figure 10. Total and regional (a) pedal plantar, and (b) pedal dorsal stresses incurred over a gait cycle during normal, level walking by a test subject wearing shoes judged "too tight" across the metatarsal heads, but otherwise deemed to be acceptably fitting. The subject evidence reduced heel and midfoot loading relative to that in the forefoot. The largest stresses applied on the dorsal aspect of the foot were evidenced on the dorsal medial aspect of the hallux and the lateral dorsal aspect of the fifth metatarsal head. A (considerably smaller) peak was also observed to occur on the medial dorsal aspect of the first metatarsal head between heel rise and toe off as weight was transferred to the contralateral limb. These results indicate that stresses above 4 psi in magnitude that are routinely applied to the dorsum of the foot over regions with prominent underlying bony structures are excessive, and can lead to discomfort and potential trauma.

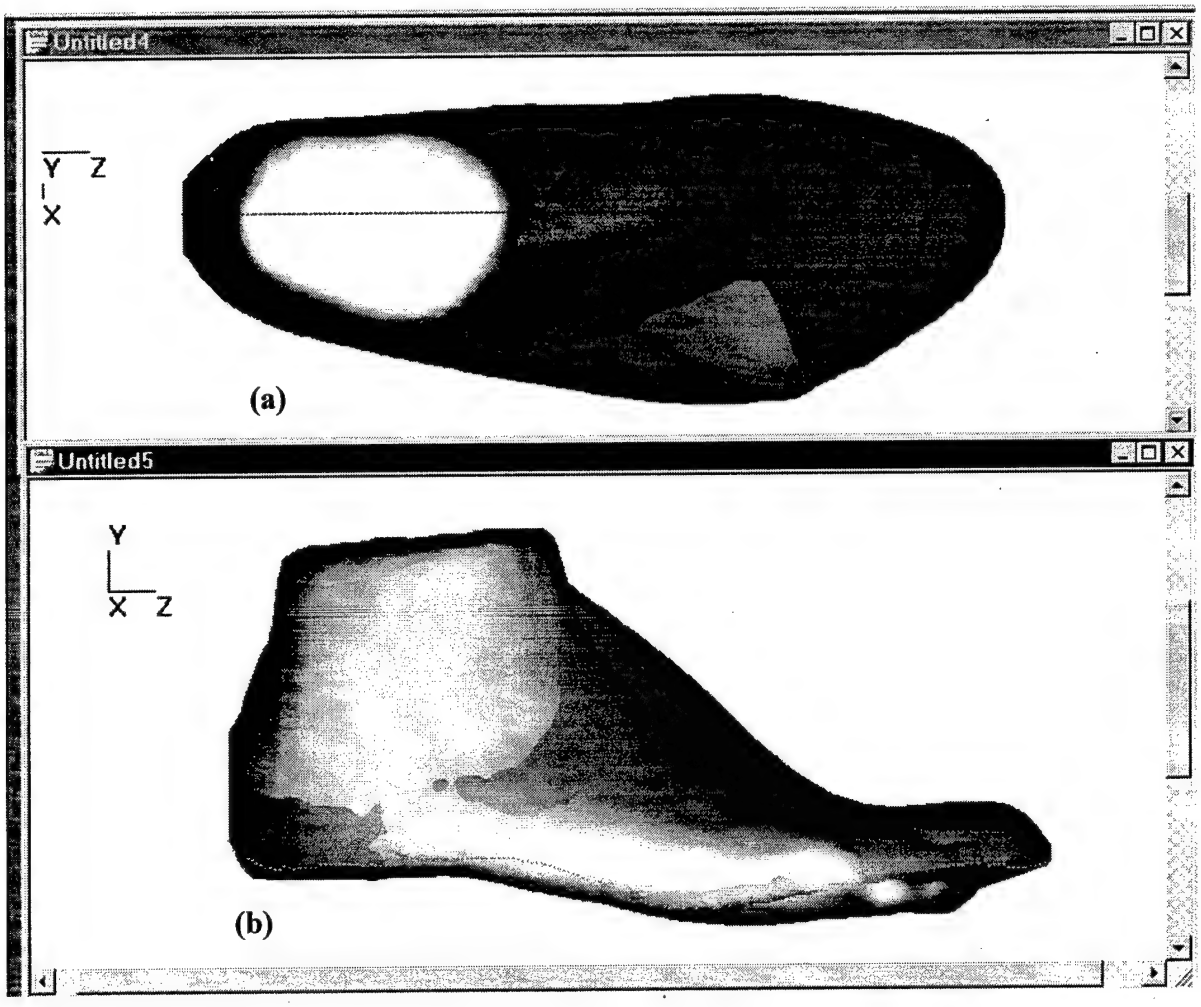

(c) Pedorthic Foot/Ankle and Footwear Last Grading Parameters

Pedorthic Grading Parameters *(mm)*	Parametric Dimension Test Subject Foot/Ankle	Parametric Dimension Military Footware Last	Dimensional Differences (Subj Foot/Ankle – Last)
Heel to toe length	243	254	–11
Heel to ball length	170	178	–8
Heel to crest length	108	117	–9
Ball width	95	87	+8
Heel width	69	61	+8
Span circumference	326	325	+1
Ball circumference	232	217	+15
Instep circumference	260	243	+17
Waist circumference	242	230	+12
Toe box height	23	26	–3
Total Volume *(cm^3)*	924	670	254

Figure 11. VA Pedorthic CAD System shaded solid **(a)** dorsal and **(b)** lateral sagittal views of the foot and ankle of a normal, healthy female subject of military service age with the "best" fitting DLA DPSC US Military Last superimposed. Non-compliant regions between the subject's foot/ankle and the Last, which are at potential risk of injury, are evident. **(c)** Set of eleven pedorthic "grading" parameters, only two or three of which are typically used to assess fit, are shown for the subject's foot and the Last.

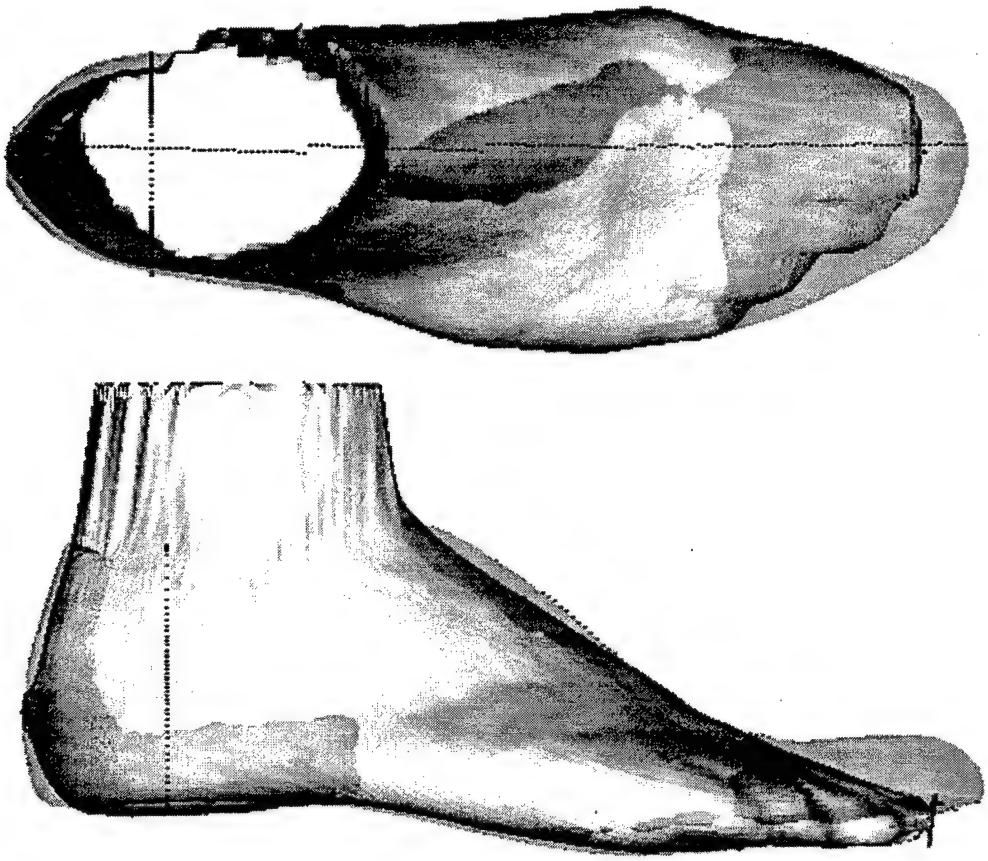

(c) Pedorthic Foot/Ankle and Footwear Last Grading Parameters

Pedorthic Grading Parameters *(mm)*	Parametric Dimension Test Subject Foot/Ankle	Parametric Dimension Military Footware Last	Dimensional Differences (Subj Foot/Ankle – Last)
Heel to toe length	232	243	-11
Heel to ball length	162	170	-8
Heel to crest length	104	113	-9
Ball width	87	79	8
Heel width	52	57	-5
Span circumference	285	293	-8
Ball circumference	214	187	27
Instep circumference	225	212	13
Waist circumference	222	207	15
Toe box height	19	24	-5
Total Volume *(cm^3)*	717	532	185

Figure 12. Shaded solid dorsal and lateral views of the scan of the foot–ankle of a normal, healthy female subject of military service age, shown with the "best" fitting DLA DPSC US Military Last superimposed. The values of the eleven most common parameters used in Last grading are also given for the subject's foot and the Last, respectively. Regions of compliance and non-compliance between the foot and the Last are evident. The subject is representative of the substantial percentage of females with narrow heels, in contrast to the subject shown in Figure 11, whose foot has a larger heel width to metatarsal ball width ratio. For the project sample population, the heel widths to ball widths measured for the subjects, normalized with respect to heel-to-ball length, evidenced weak to negligible correlation ($R^2 = 0.2509$). This elucidates the significant variation that exists among peoples' pedal structure and dimensions, and thus the resulting difficulty inherent in providing properly fitting and functioning footwear for **all** personnel.

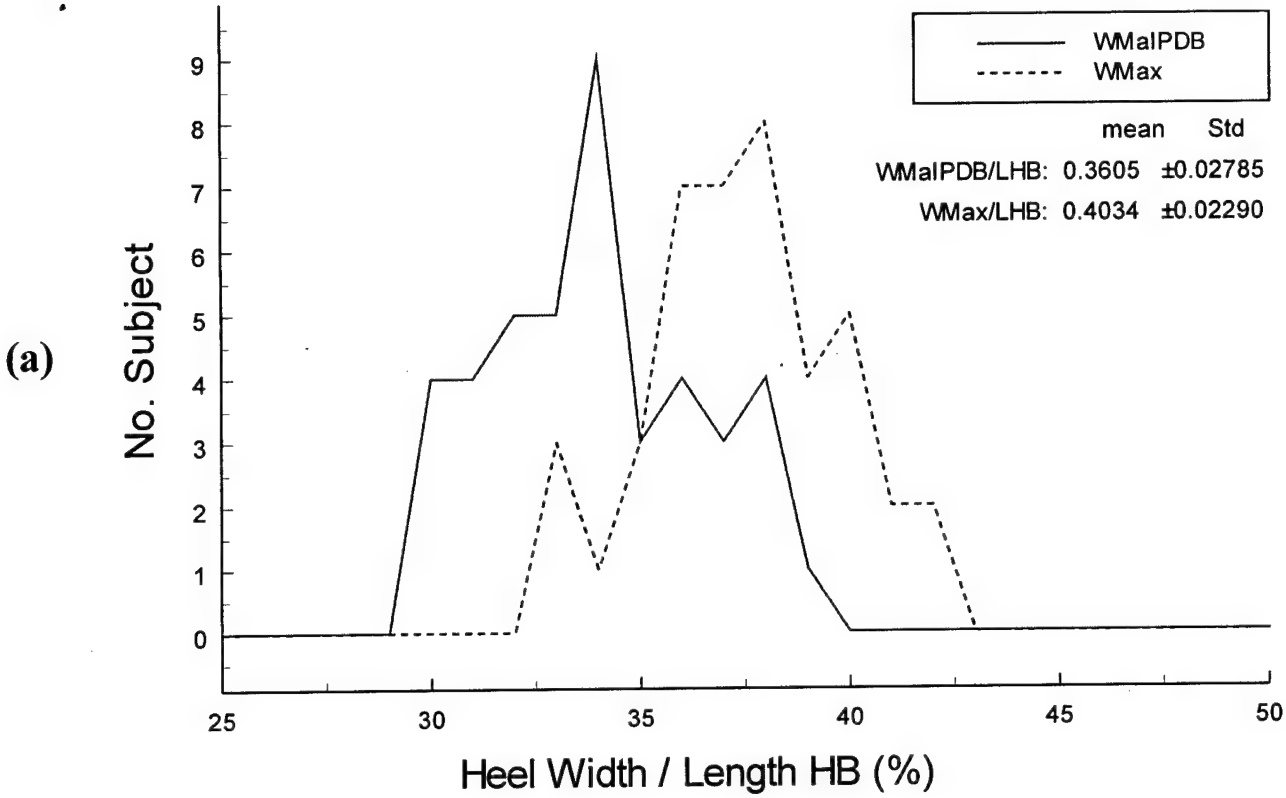

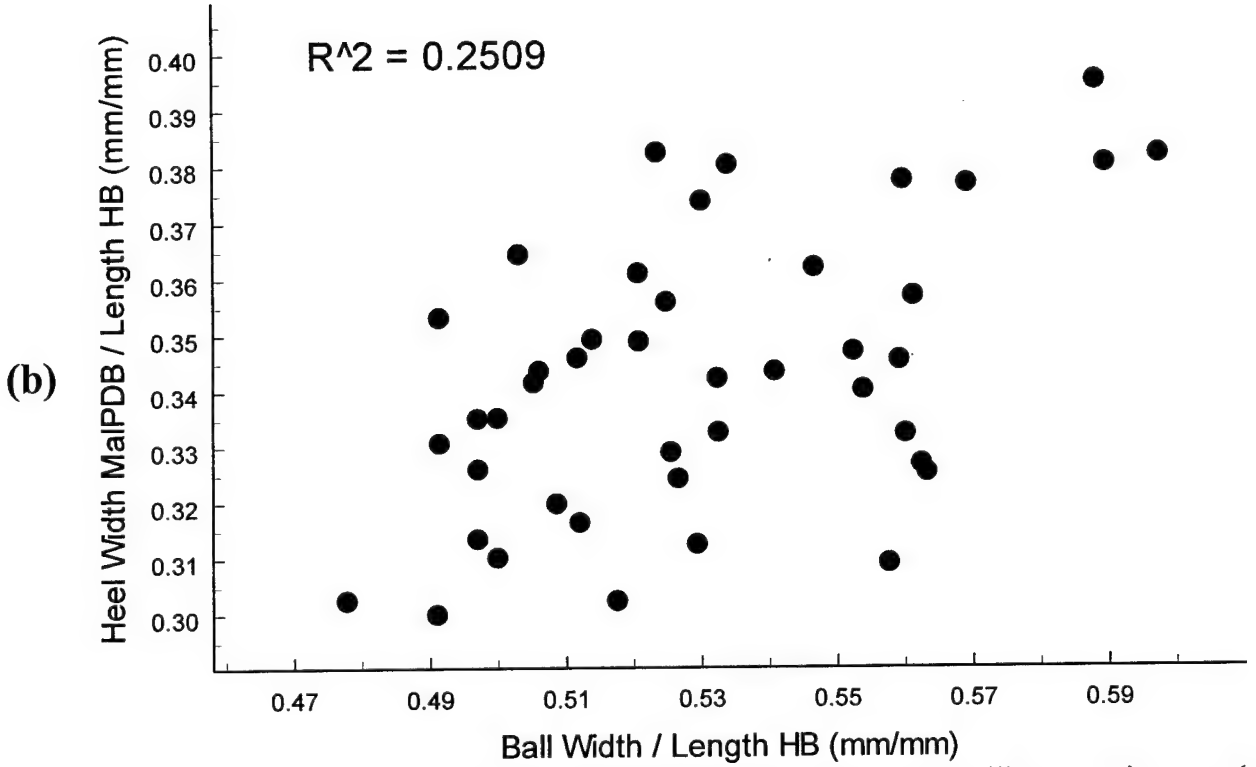

Figure 13. Heel width measurements for 43 normal, healthy females of military service age. **(a)** Heel widths for the subjects measured posterior to the medial malleolus at its distal border (W_{MalPDB}), together with maximum heel widths (W_{Max}) measured in the same cross section, normalized with respect to the subject's heel-to-ball center length (L_{HB}). The resulting distributions are (approximately) Gaussian, and have sizable dispersions ($\pm\sigma_W$). Differences between the W_{MalPDB} and W_{Max} distributions reflect significant differences in the heel contours between different subjects. Calculations further show only mild correlation between W_{MalPDB} and W_{Max} ($R^2_{W_{MalPDB}-W_{Max}} = 0.6120$) **(b)** Plot of the regression between normalized heel width W_{MalPDB}/L_{HB} and normalized ball width W_{Ball}/L_{HB} shows wide dispersion with small to negligible correlation, $R^2_{W_{MalPDB}-W_{Ball}} = 0.2509$, reflecting the non-algebraically scaled structure of the foot–ankle among different individuals.

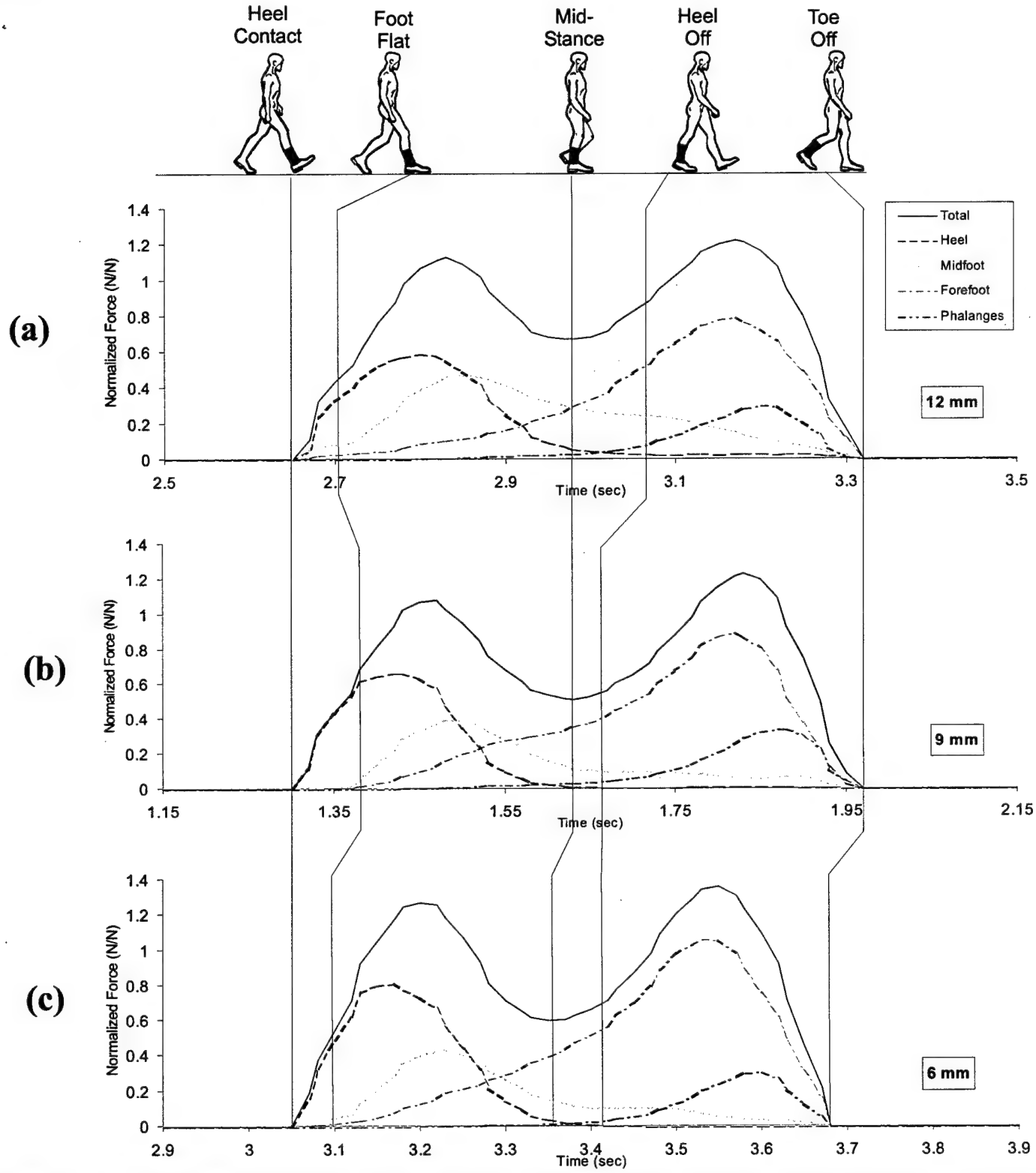

Figure 14. Biomechanical studies of the effects of arch supports on pedal plantar stresses. Total and regional plantar stresses over a typical gait cycle during normal, level walking at a subject selected speed of 1.8 m/sec, are shown for a normal, healthy test subject of military service age wearing well-fitting oxford shoes with 50 Shore hardness durometer RTV rubber scaphoid pads (arch supports). The pads were matched to the subject's longitudinal and transverse arch dimensions, with thickness as a parameter. The resultant stresses incurred in the subject's foot are shown for pad thicknesses of: **(a)** 12 mm; **(b)** 9 mm; and **(c)** 6 mm, respectively. The subject rated the level of comfort afforded by the respective pads as: **(a)** "uncomfortable/painful;" **(b)** "somewhat uncomfortable-to-tolerable;" and **(c)** "comfortable." The resultant segmental loads, show that with the 12 mm thickness pad, appreciable loading could be offset from the forefoot to the arch. This correspondingly was reduced as the pad thickness was decreased. The differences in pressures measured for the 9 mm versus 6 mm thickness pads were not large, however, their effects on the subject's level of comfort were significant.

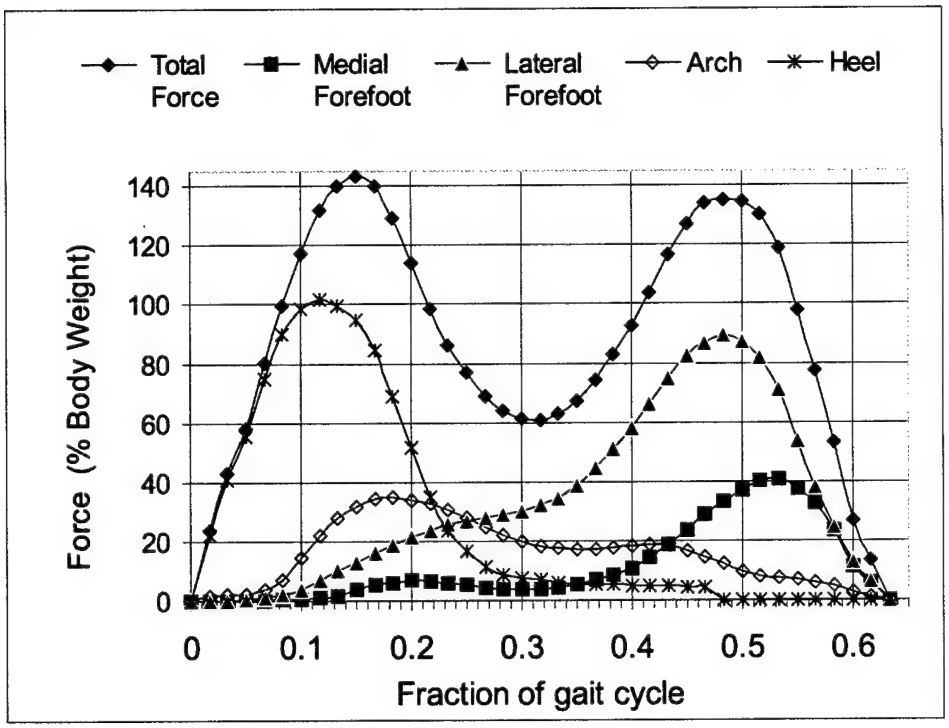

(a)

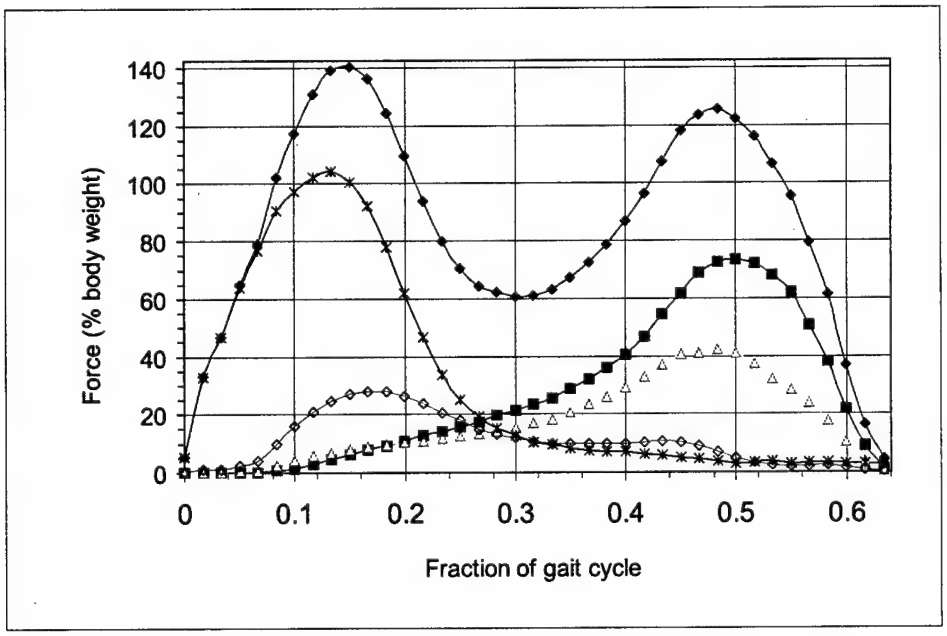

(b)

Figure 15. Biomechanical studies of the effects of shoe outer sole wedges on pedal/footwear interface stress magnitudes, spatial distribution, temporal duration, and lower limb kinematics. Total and regional plantar stresses over a typical gait cycle during normal, level walking at a subject selected speed of 1.8 m/sec, are shown for the right foot of a normal, healthy test subject of military service age wearing well-fitting oxford shoes with a lateral sole wedge. Results are shown for wedges of: **(a)** 0 mm in thickness (no wedge); **(b)** 8 mm in thickness;

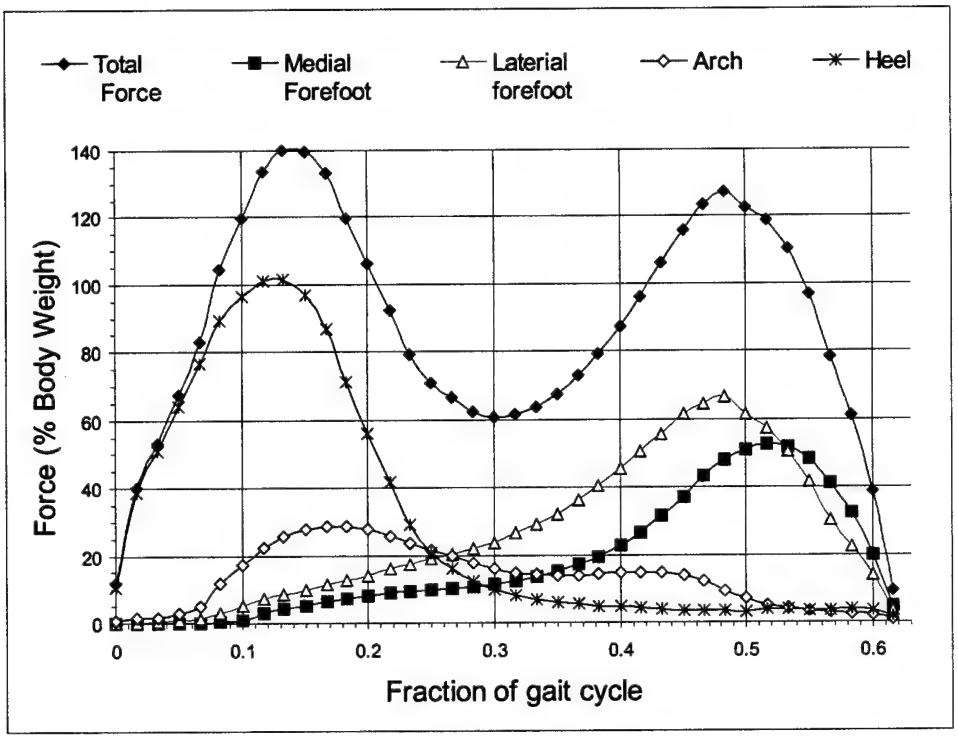

(c)

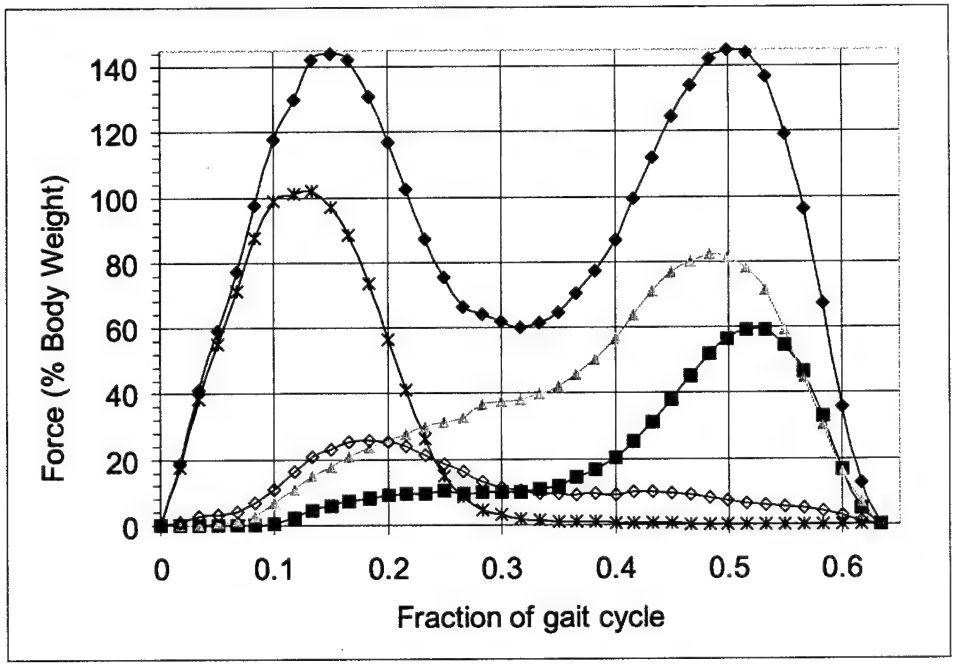

(d)

Figure 15. (cont.) (c) 4 mm in thickness; and **(d)** 2 mm in thickness. As seen, an 8mm sole wedge effectively reduces forefoot loading on the respective side of application. Wedges of decreasing thickness were found to correspondingly produce reduced effects on loading, until at 2mm thickness their effect was negligible.

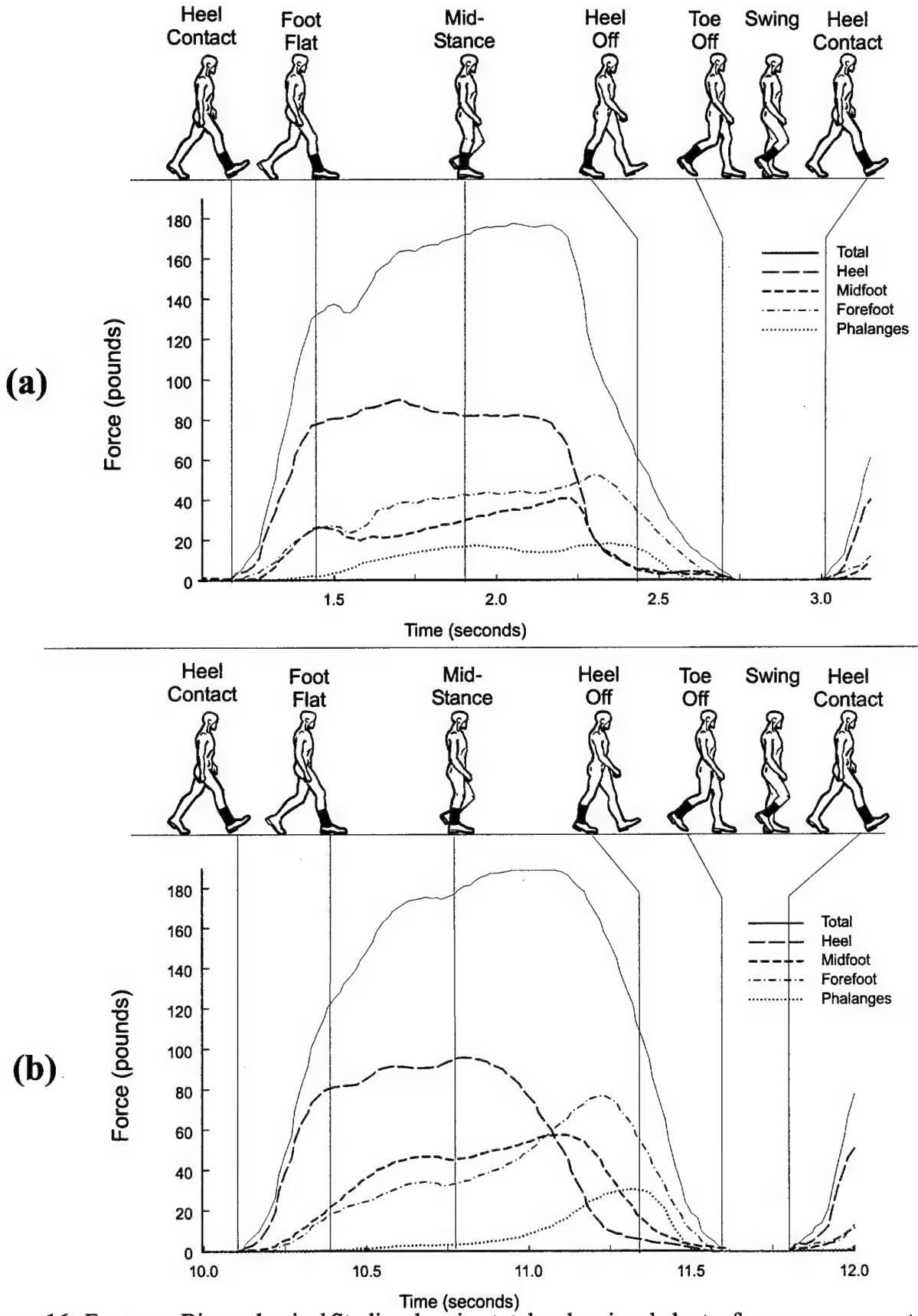

Figure 16. Footwear Biomechanical Studies showing total and regional plantar force measurements versus time from the central gait cycle in a 10 m level walking trial at user selected walking speed, for the right foot of a test diabetic subject with a peripheral neuropathy wearing oxford style shoes with: **(a)** "normal" width outer soles and heels; and **(b)** ½" extended width outer soles and heels. Non-demarcated heel contact-to-foot flat, with prolonged loading of the heel and mid-foot regions, and lengthened and reduced amplitude loading of the forefoot, indicative of a festinating gait is evident in the "normal" width sole and heel shoes. In the extended width sole and heel shoes the subject's gait is slightly improved, with heel contacttofoot flat, midstance, and heel risetotoe off gait phases being more clearly defined, and the duration of heel and midfoot loading reduced, indicating a more controlled, stabler, energy efficient gait.

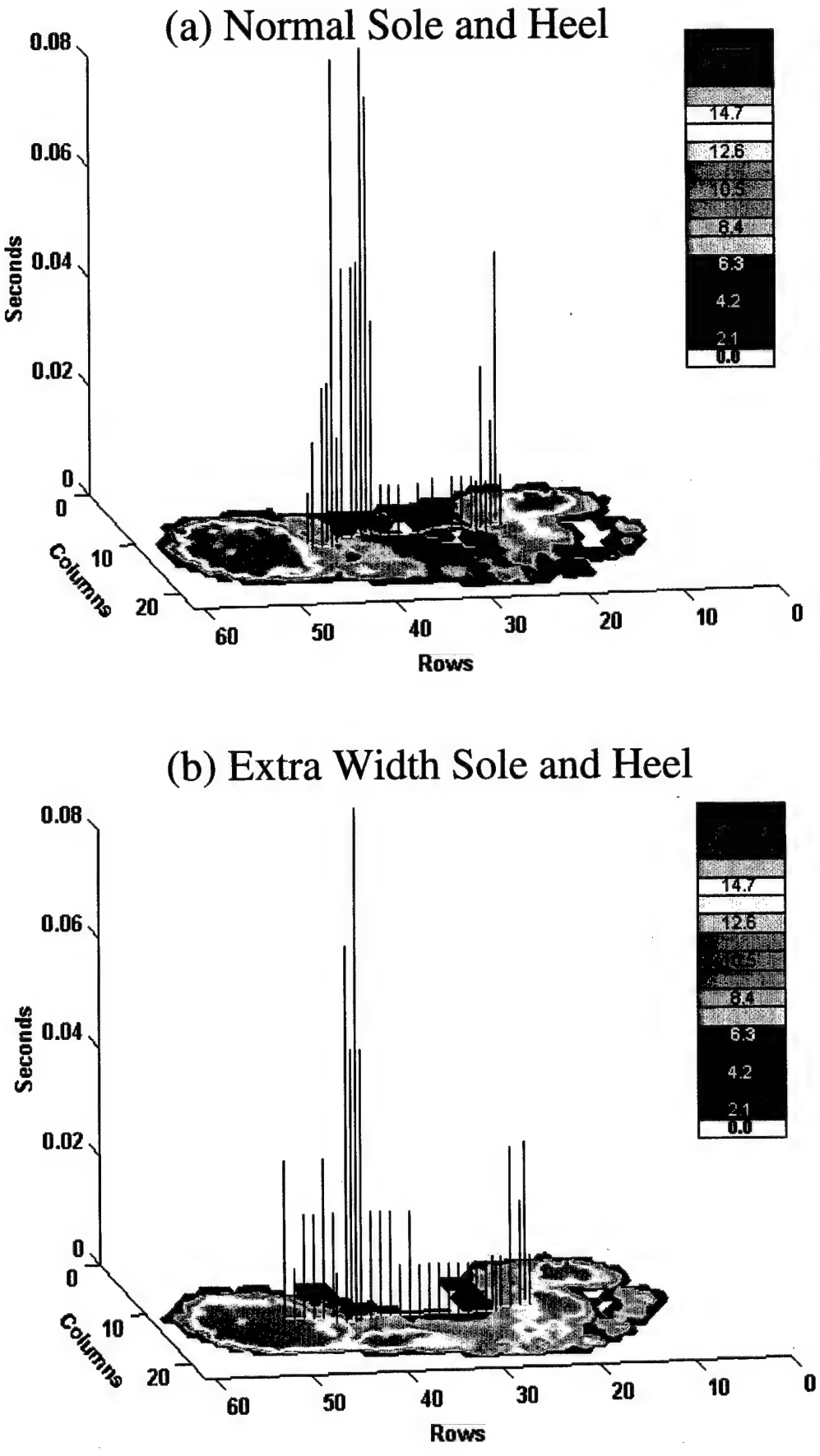

Figure 17. Peak plantar pressures over a gait cycle in the 10 m level walking trial of the neuromuscular test subject shown in Figure 16. Measurements were acquired using individual sensel calibrated, 960 element, FScan FVR insole transducers, sampled at 100 Hz. Pressures are shown color encoded by magnitude. Center of pressure (COP) trajectories are shown as a white line in the (x,y)–plane, with corresponding segmental temporal loading durations plotted along the z–axis. **(a)** In the shoes with standard width outer soles and heels, the subject is seen to initiate floor contact flatfooted, maintaining much of his body weight back on his heel throughout the weight transfer and midstance phases of gait. The subject's COP is seen to wander erratically, reflecting difficulty in neuromuscular control, and decreased stability. **(b)** With the extended width sole and heel shoes, loading is seen to be distributed more evenly over the subject's foot; he has more clearly demarcated heel contact and heel rise–to–toe off gait phases; and his COP trajectory is much smoother, indicating a stabler gait.

PARAMETER	tot/Left	Right
Leg Length(cm)	89.	89.
Step Time(sec)	.992	.972
Step Length(cm)	28.444	31.469
Step Extremity(ratio)	.32	.35
Cycle Time(sec)	1.963	1.982
Stride Length(cm)	59.94	61.359
HH Base Support(cm)	15.073	15.139
Swing Time(sec)	.565	.492
Stance Time(sec)	1.398	1.49
Single Supp. Time(sec)	.492	.565
Double Supp. Time(sec)	.912	.898
Swing % of Cycle	28.8	24.8
Stance % of Cycle	71.2	75.2
Single Supp % Cycle	25.1	28.5
Double Supp % Cycle	46.5	45.3
Toe In / Out	18.1	21.3

PARAMETER	
Step Count	24.
Distance	718.95
Ambulation Time	23.56
Velocity	30.5
Normalized Velocity	61.1
Cadence	.34
Step Time Differential	.02
Step Length Differential	3.025
Cycle Time Differential	.019
Functional Amb. Profile	55.

(a) Standard Shoes

PARAMETER	tot/Left	Right
Leg Length(cm)	89.	89.
Step Time(sec)	.978	1.09
Step Length(cm)	29.106	32.063
Step Extremity(ratio)	.33	.36
Cycle Time(sec)	2.082	2.078
Stride Length(cm)	62.3	61.063
HH Base Support(cm)	10.536	10.332
Swing Time(sec)	.554	.58
Stance Time(sec)	1.528	1.498
Single Supp. Time(sec)	.58	.554
Double Supp. Time(sec)	.948	.945
Swing % of Cycle	26.6	27.9
Stance % of Cycle	73.4	72.1
Single Supp % Cycle	27.9	26.7
Double Supp % Cycle	45.5	45.5
Toe In / Out	16.8	24.1

PARAMETER	
Step Count	23.
Distance	701.97
Ambulation Time	23.74
Velocity	29.6
Normalized Velocity	58.1
Cadence	.33
Step Time Differential	.112
Step Length Differential	2.957
Cycle Time Differential	.004
Functional Amb. Profile	56.

(b) Wide Soles

Figure 18. GaitRite Electronic Walkway measurements over the 10 m level walking trial at user selected speed for the neuromuscular test subject in Figures 16 and 17: **(a)** in standard width sole and heel shoes, and **(b)** in extended width sole and heel shoes. In the extended width sole and heel shoes the subject's stride length is slightly increased; his mediolateral gait base decreased, and his COM mediolateral accelerations decreased — all indicative of an improved, more stable gait.

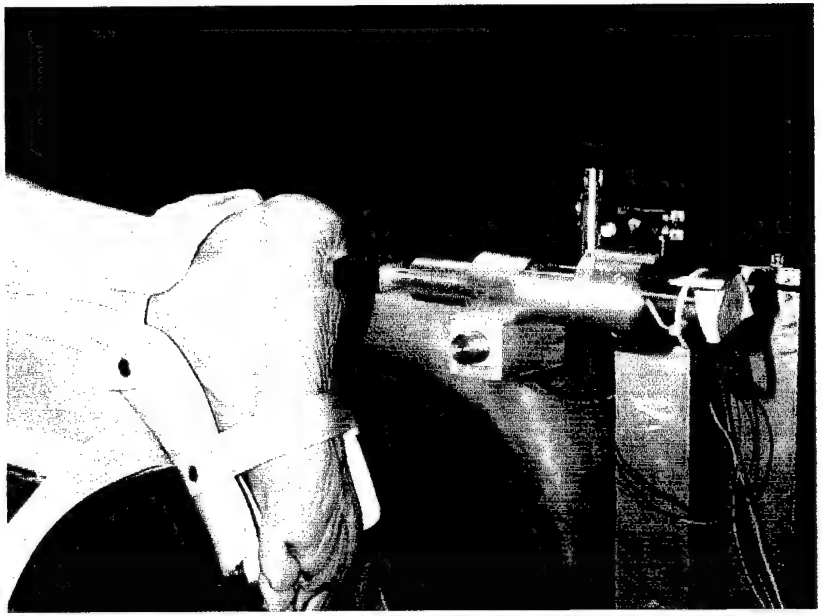

(a)

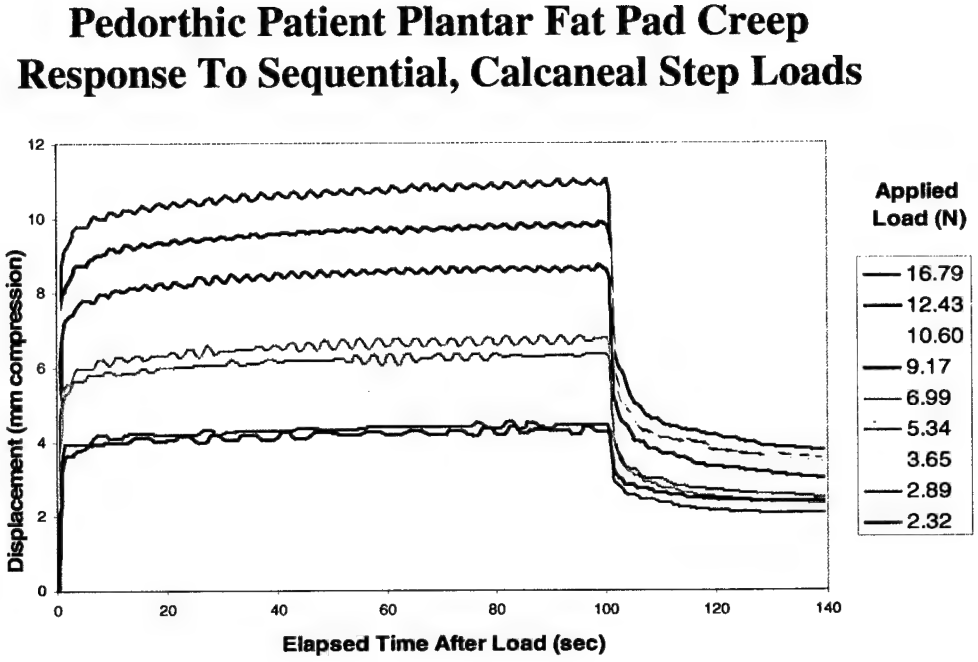

(b)

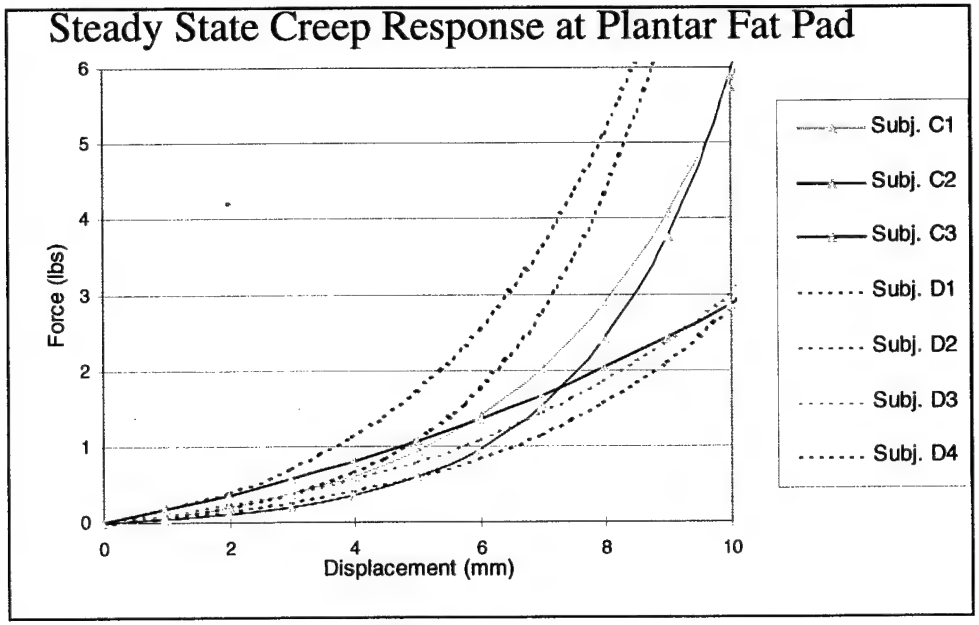

(c)

Figure 19. **(a)** Measurement of the mechanical properties of a test subject's pedal fat pad with the VA NYHHS optoelectromechanical tissue indentor. As shown, subjects are mechanically "locked" in place relative to the indentor frame to mitigate "movement noise". **(b)** Tissue creep responses at nine step force loads of increasing magnitude, sequentially applied to the plantar fat pad. **(c)** Resulting Force-Displacement plots of the steady state creep response of the pedal plantar fat pads for 3 normal subjects, and 4 neuropathic diabetic subjects.

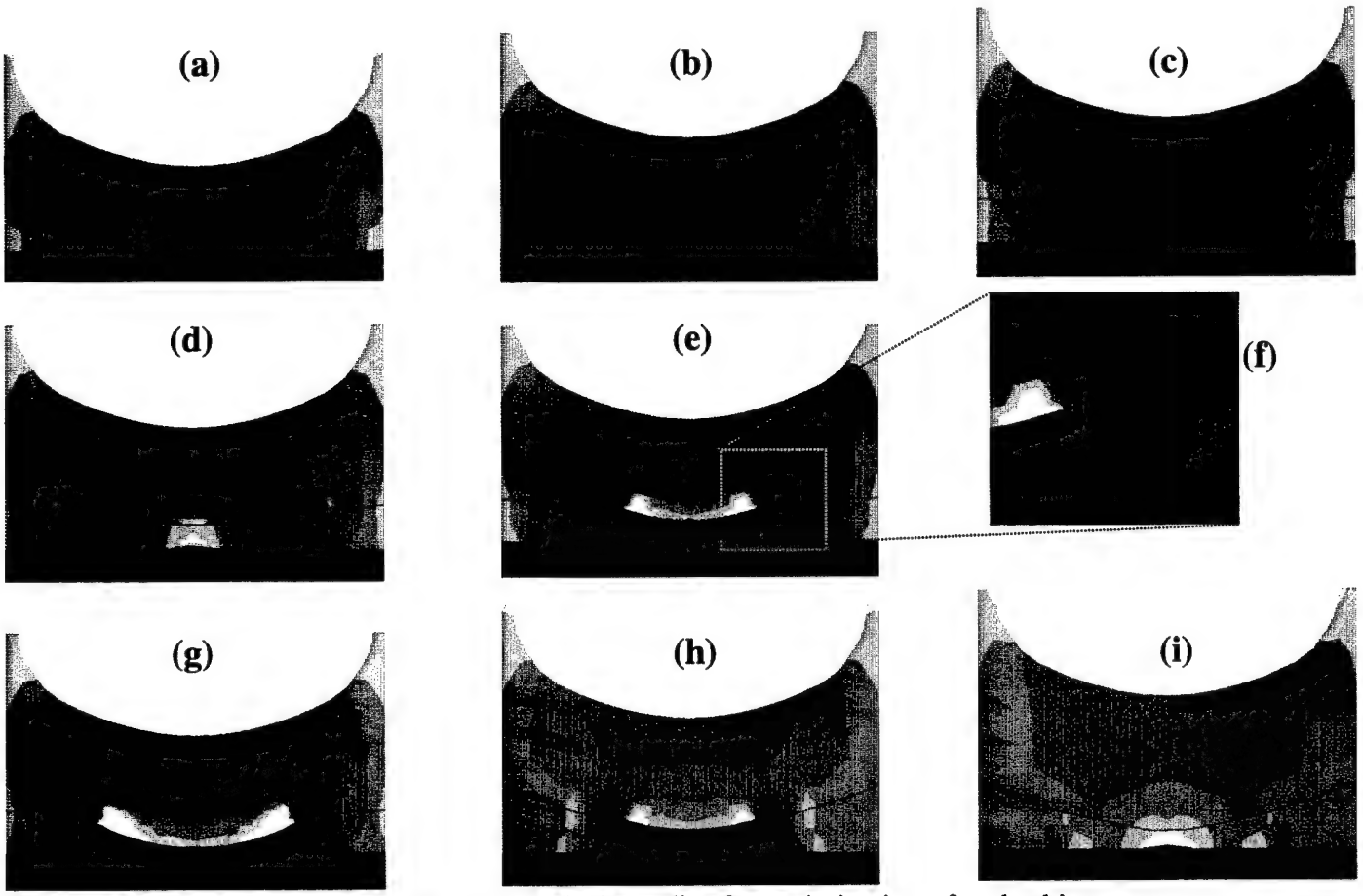

Figure 20. Finite element modeling and analysis studies for optimization of pedorthic treatment of podalgia/plantar fasciitis. Mid-calcaneal, frontal cross sections of the foot of a test subject showing FEA predicted vertical stress incurred, as a function of pedorthic insole material stiffness and design geometry, when the subject stands on a flat, rigid surface, applying a vertical load of 200 Newtons (approximately ¼ body weight) through his talus and calcaneous. All insoles in their unloaded state are 5 mm thick at center. **(a)** Tissue stress distribution incurred with the subject standing barefoot without a pedorthosis. **(b)** Tissue stress distribution incurred with the subject standing on a non-contoured, generic insole, with material stiffness equivalent to that of his pedal tissues. **(c)** Stress distribution incurred when standing on a non-contoured insole with material stiffness six times that of his pedal tissue. **(d)** Stress distribution produced by standing on a non-contoured, generic insole, six times pedal tissue stiffness, with a conical relief 25 mm in base diameter and 2.5 mm deep cut out of the bottom of the insole under the heel. **(e)** Stress distribution produced by standing on a non-contoured insole, six times pedal tissue stiffness, with a 14 mm diameter cylindrical relief cut out of the insole under the heel. **(f)** Enlarged inset of case (e) showing the increase in stress magnitudes due to the Dunnel effect from large gradients in stiffness of adjoining materials at the tissue–insole–relief junction. **(g)** Stress distribution produced with a non-contoured insole, six times pedal tissue stiffness, with a 20 mm diameter cylindrical relief cut out under the heel. **(h)** Stress distribution produced with an insole six times pedal tissue stiffness, and custom made to match the subject's pedal contours, with a 14 mm diameter cylindrical relief cut out under the heel. **(i)** Stress distribution produced with a custom contoured insole, six times the pedal tissue stiffness, with a conical relief 25 mm in base diameter and 2.5 mm deep cut out under the heel, and with the additional condition that rheological displacement of pedal soft plantar tissues relative to the calcaneous is constrained (as achieved by extending the borders of the insole proximally around the fat pad to hold it in place). As clearly evident, only in this latter case are tissue stresses and stress gradients reduced appreciably. *(See Table 3 for a quantitative tabulation of results.)*

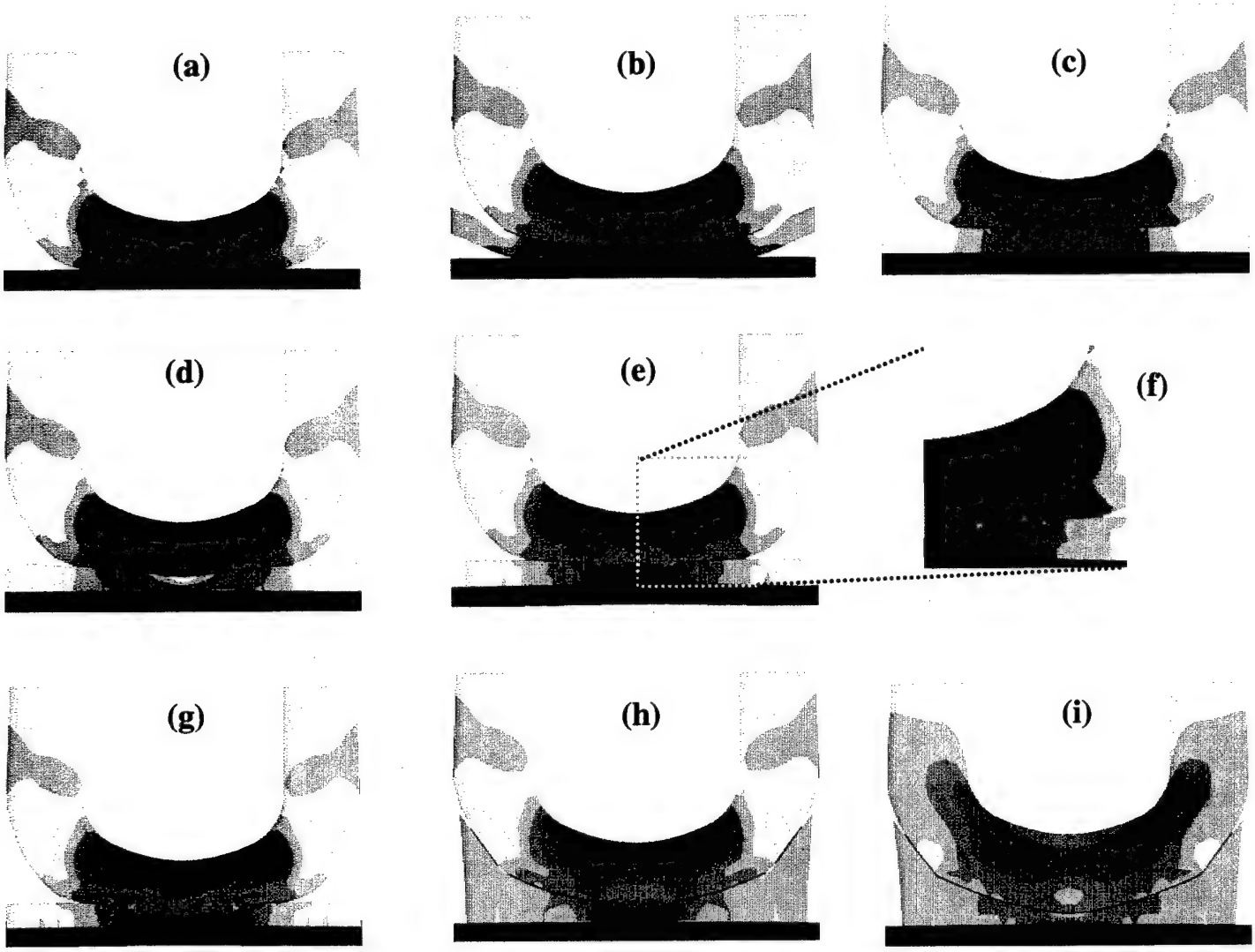

Figure 21. Finite element modeling and analysis studies for optimization of pedorthic treatment of podalgia/plantar fasciitis. FEA predicted tissue total vertical strains at the mid-calcaneal, frontal cross section of the test subject's foot in Figure 20, standing on a flat, rigid surface supporting a 200 Newton vertical load through his calcaneous and talus. **(a)** Tissue strains incurred standing barefoot without a pedorthosis. **(b)** Tissue strains incurred when standing on a non-contoured, generic insole with material stiffness equivalent to that of the subject's pedal tissues. **(c)** Strains incurred when standing on a non-contoured insole with material stiffness six times that of pedal tissue. **(d)** Tissue strains produced by standing on a non-contoured insole, six times pedal tissue stiffness, with a conical relief 25 mm in base diameter and 2.5 mm deep cut out of the bottom of the insole under the heel. **(e)** Strains produced by standing on a non-contoured insole, six times pedal tissue stiffness, with a 14 mm diameter cylindrical relief cut out of the insole under the heel. **(f)** Enlarged inset of case (e) showing the strains and strain gradients produced adjacent to the insole relief border. **(g)** Strains produced with a non-contoured insole, six times pedal tissue stiffness, with a 20 mm diameter cylindrical relief cut out under the heel. **(h)** Strains produced with an insole six times pedal tissue stiffness, and custom fabricated to match the subject's pedal contours, with a 14 mm diameter cylindrical relief cut out under the heel. **(i)** Strains produced with a custom contoured insole, six times pedal tissue stiffness, with a conical relief 25 mm in base diameter and 2.5 mm deep cut out under the heel, and with the additional condition that rheological displacement of pedal soft plantar tissues relative to the calcaneous is constrained (as achieved by extending the borders of the insole proximally around the fat pad to hold it in place). As evident, only in this latter case are tissue strains reduced appreciably.

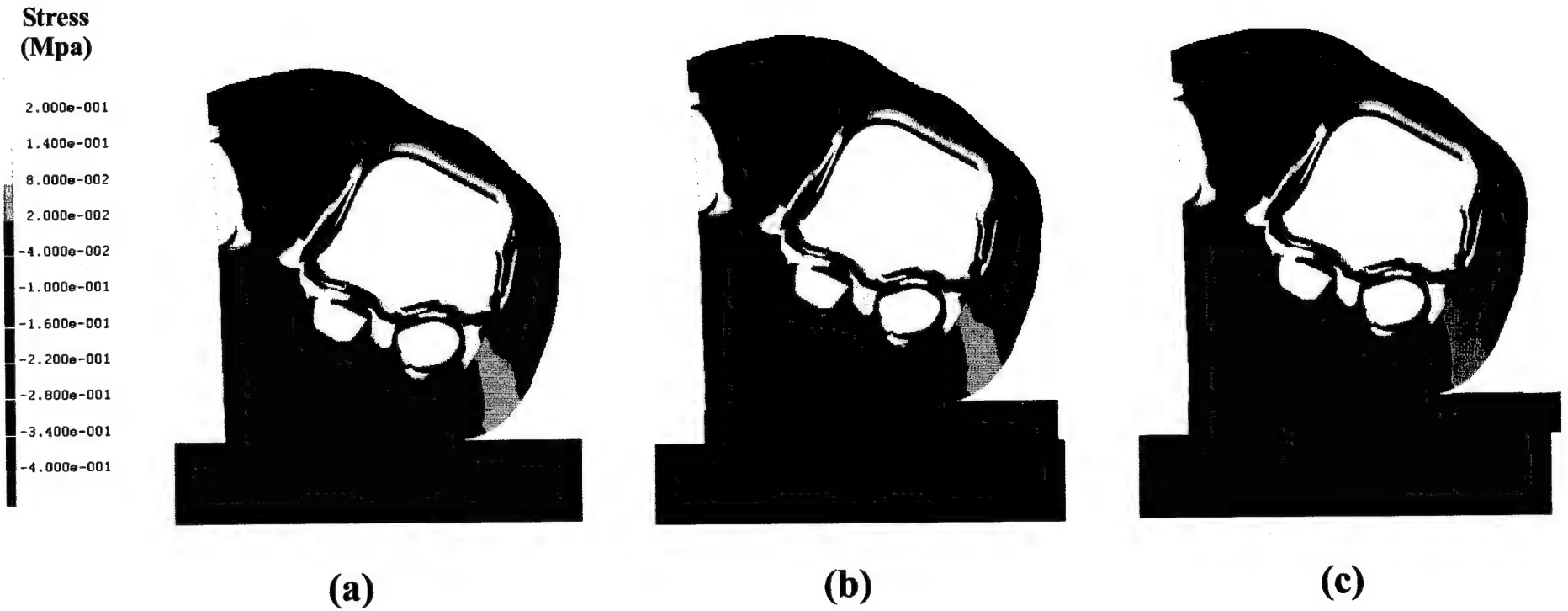

Figure 22. FEA predicted vertical Cauchy stresses produced at the 1st metatarsal head of a test subject standing: **(a)** barefoot on the floor; **(b)** on an insole made from Latex impregnated cork (with 80 Shore hardness durometer); and **(c)** on a poron insole of 30 Shore hardness durometer. Differences in the resulting peak stresses produced in the pedal tissues are seen to be minimal, with the spatial distribution of the stress in the pedal tissues supported on the softer poron being generally slightly lower in magnitude and more dispersed.

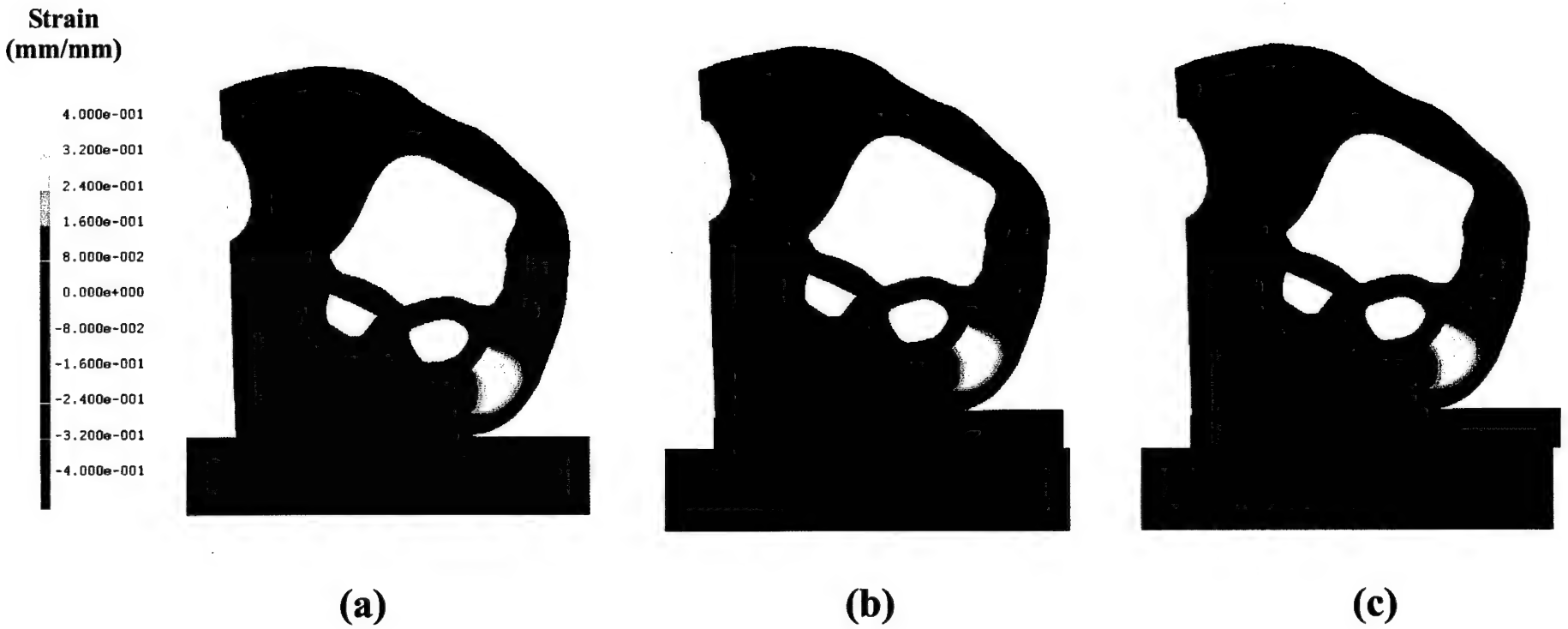

Figure 23. FEA predicted vertical Green strains produced at the 1st metatarsal head of a test subject standing: **(a)** barefoot on the floor; **(b)** on an insole made from Latex impregnated cork (with 80 Shore hardness durometer); and **(c)** on a poron insole of 30 Shore hardness durometer. The strains produced in the pedal tissues supported by the insoles are slightly smaller than in the barefoot case. The pedal tissue strains supported on the softer poron are generally slightly lower in magnitude and more dispersed.

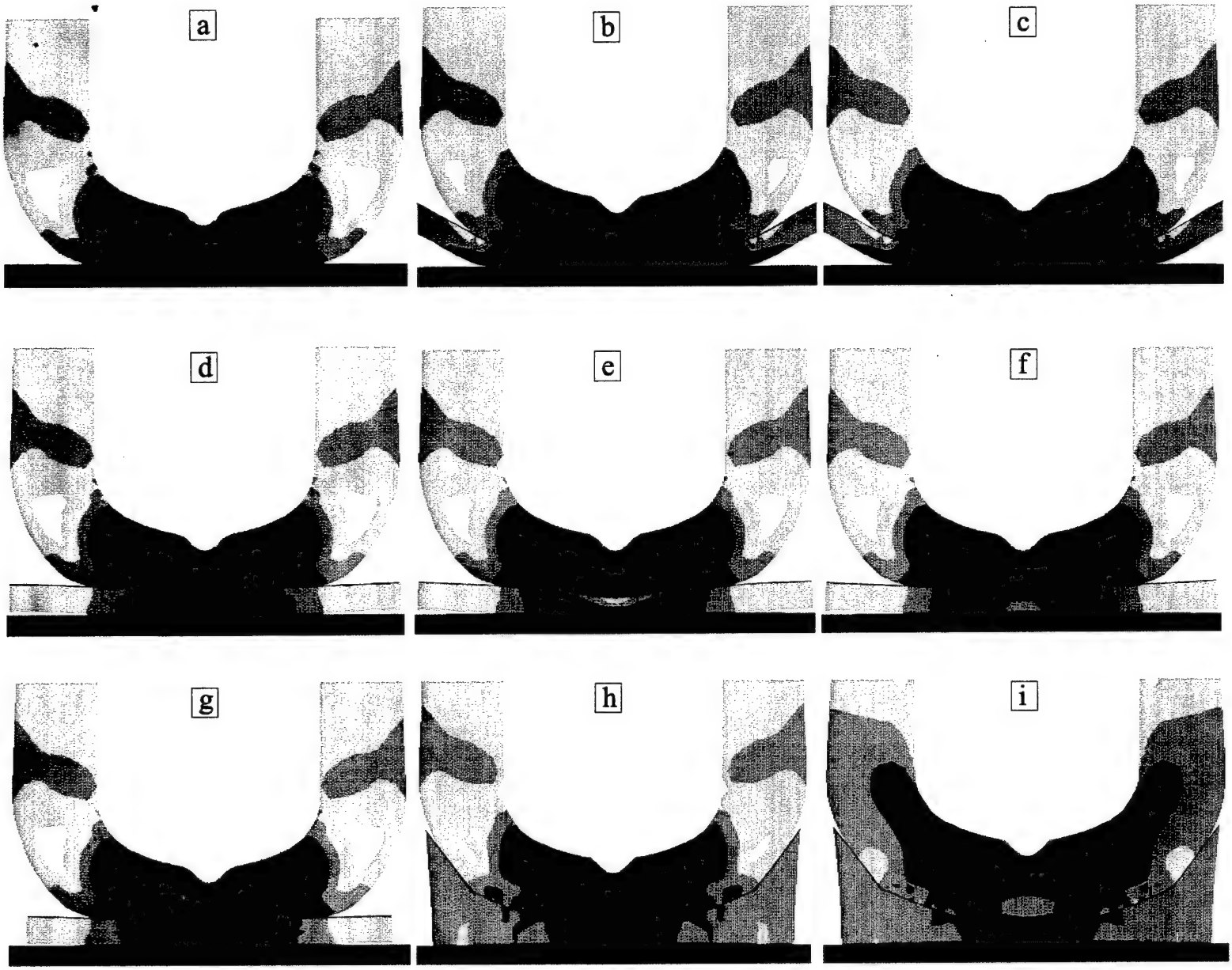

Figure 24. Finite element modeling and analysis studies for optimization of pedorthic treatment for calcaneal osteophytes. FEA predicted tissue total vertical strains at the mid-calcaneal, frontal cross section of the foot of a test subject with a vertical heel spur, standing on a flat, rigid surface, applying a 200 Newton vertical load through his talus and calcaneous. Tissue strains are shown as a function of pedorthic insole material stiffness and design geometry. All insoles are 5 mm thick at center in their unloaded state. **(a)** Tissue strains incurred with the subject standing barefoot without a pedorthosis. **(b)** Tissue strains incurred when standing on a non-contoured, generic insole with material stiffness equivalent to that of the subject's pedal tissues. **(c)** Strains incurred when standing on a non-contoured insole with material stiffness 2.5 times that of pedal tissue. **(d)** Tissue strains produced by standing on a non-contoured insole, six times pedal tissue stiffness. **(e)** Tissue strains produced by standing on a non-contoured insole, six times pedal tissue stiffness, with a conical relief 25 mm in base diameter and 2.5 mm deep cut out of the top of the insole under the heel. **(f)** Tissue strains produced by standing on a non-contoured insole, six times pedal tissue stiffness, with a conical relief 25 mm in base diameter and 2.5 mm deep cut out of the bottom of the insole under the heel. **(g)** Strains produced by standing on a non-contoured insole, six times pedal tissue stiffness, with a 14 mm diameter cylindrical relief cut out of the insole under the heel. **(h)** Strains produced with an insole six times pedal tissue stiffness, and custom fabricated to match the subject's pedal contours, with a 14 mm diameter cylindrical relief cut out under the heel. **(i)** Strains produced with a custom contoured insole, six times pedal tissue stiffness, with a 14 mm diameter cylindrical relief cut out under the heel, and with the additional condition that rheological displacement of pedal soft plantar tissues relative to the calcaneous is constrained (as achieved by extending the borders of the insole proximally around the fat pad to hold it in place). Only in the latter case are pedal tissue strains reduced appreciably. *(See Table 4 for a quantitative tabulation of results.)*

Plastic Insole Material Stress-Strain Characteristics

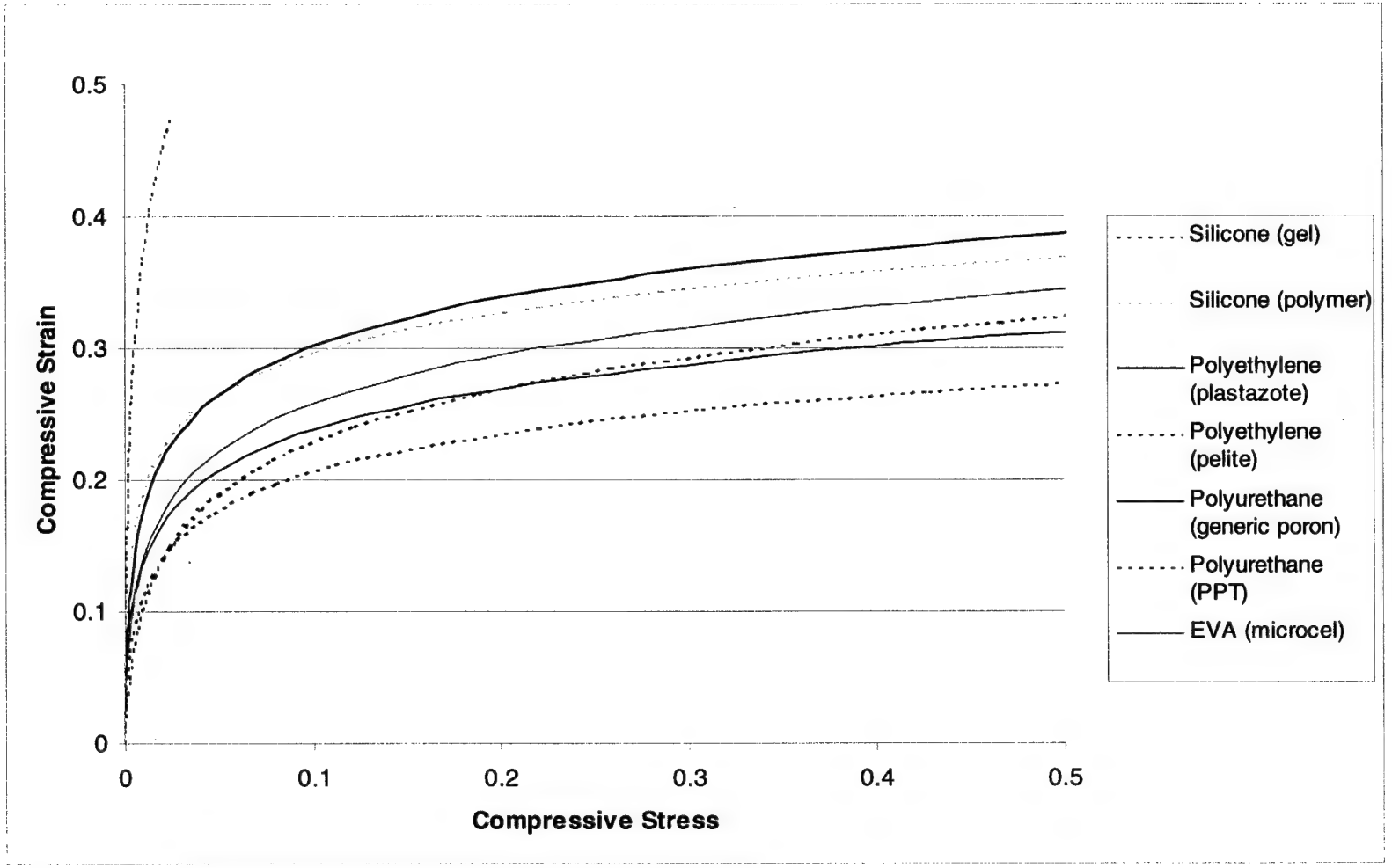

Figure 25. Nonlinear stress-strain characteristics of seven plastic materials commonly used in fabrication of orthopedic insoles.

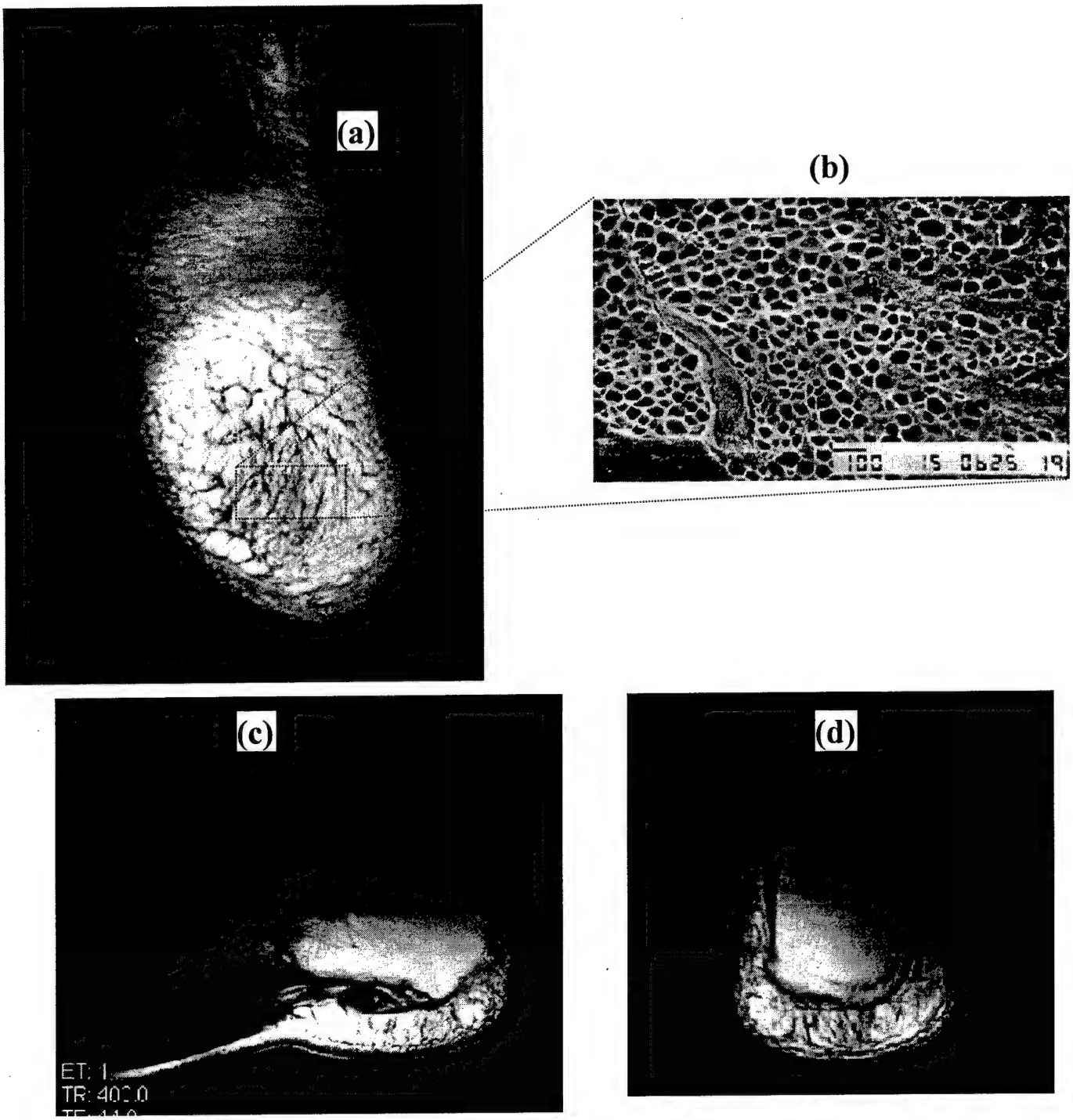

Figure 26. Magnetic resonance images of a test subject's foot in an unloaded state, showing: **(a)** a longitudinal cross section distal to the calcaneous; **(b)** a magnified histological section of the plantar fat pad under the calcaneous, showing the individual, "honey comb" like septae that dampen and disperse pedal loads; **(c)** a sagittal cross section through the mid-foot showing the morphology of the fat pad, plantar aponeurosis, calcaneous, and talus; and **(d)** a frontal cross section through the mid-calcaneous showing the relative structure of the fat pad, with axial alignment of the septae directly under the calcaneous for damping of impact loads, and gradual transition of the septal alignment to a convoluted pattern near the calcaneal borders serving to disperse plantar loading.

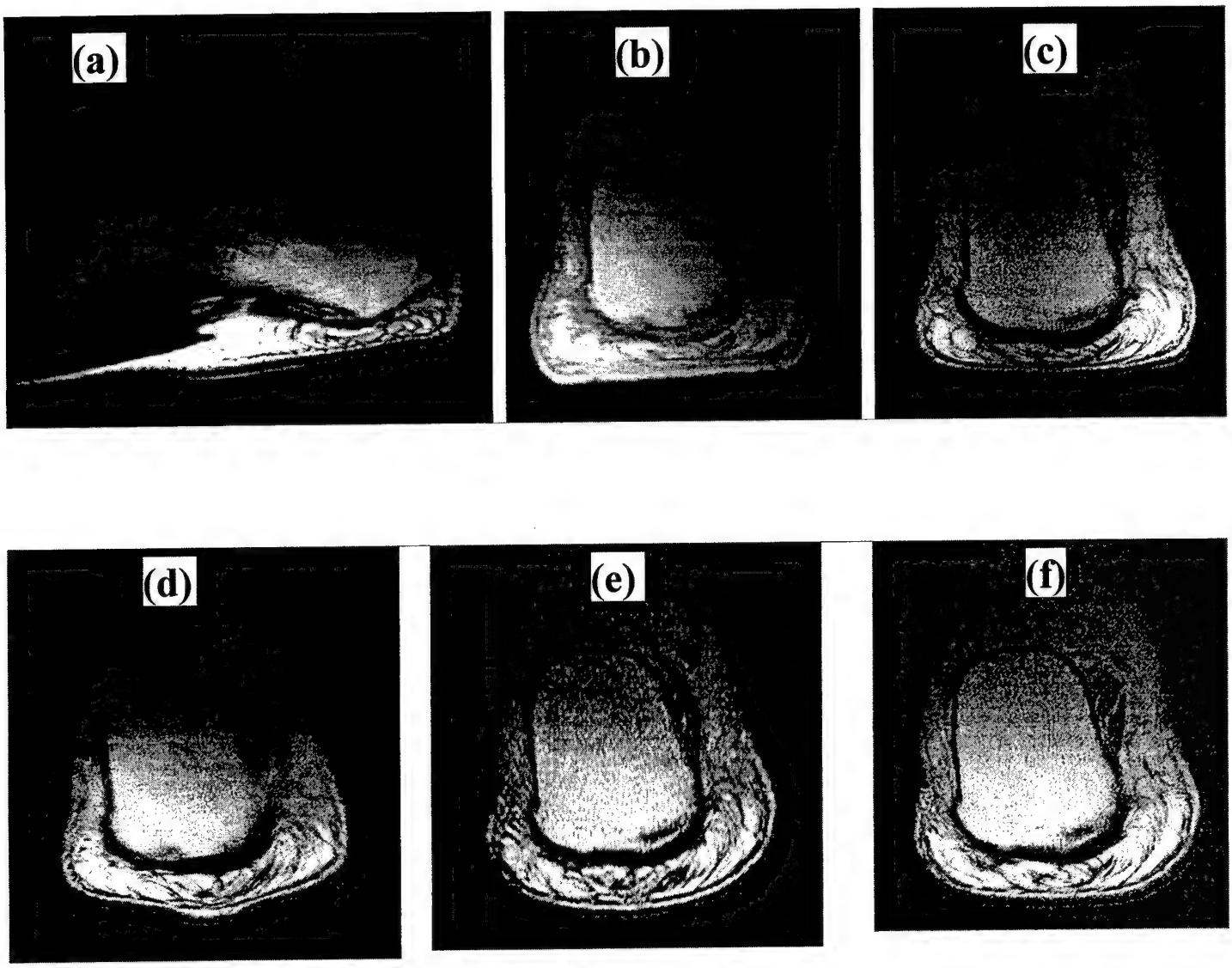

Figure 27. Magnetic resonance images of the test subject's foot in Figure 16 with a 200 Newton load applied axially through the tibia, talus, and calcaneous. **(a)** Sagittal cross section of the subject's foot axially loaded without a pedorthosis. **(b)** Frontal cross section through the mid-calcaneous of the subject's bare foot under axial load. **(c)** Frontal cross section of the subject's foot under axial load while supported on a generic, non-contoured insole, approximately six times his pedal tissue stiffness. **(d)** Frontal cross section of the subject's foot under axial load while supported on a generic, non-contoured insole, approximately six times his pedal tissue stiffness, with a 14 mm diameter cylindrical relief cut out under the heel. **(e)** Frontal cross section of the subject's foot under axial load while supported on a custom contoured insole designed to match his unloaded pedal tissue shape, approximately six times his pedal tissue stiffness. **(f)** Frontal cross section of the subject's foot under axial load while supported on an insole approximately six times his pedal tissue stiffness, custom contoured to match his unloaded pedal shape, with borders extending proximally, constraining displacement of his pedal plantar fat pad. The tissue strains incurred with the custom contoured insoles are seen to be measurably less than with the non-contoured, generic insoles.

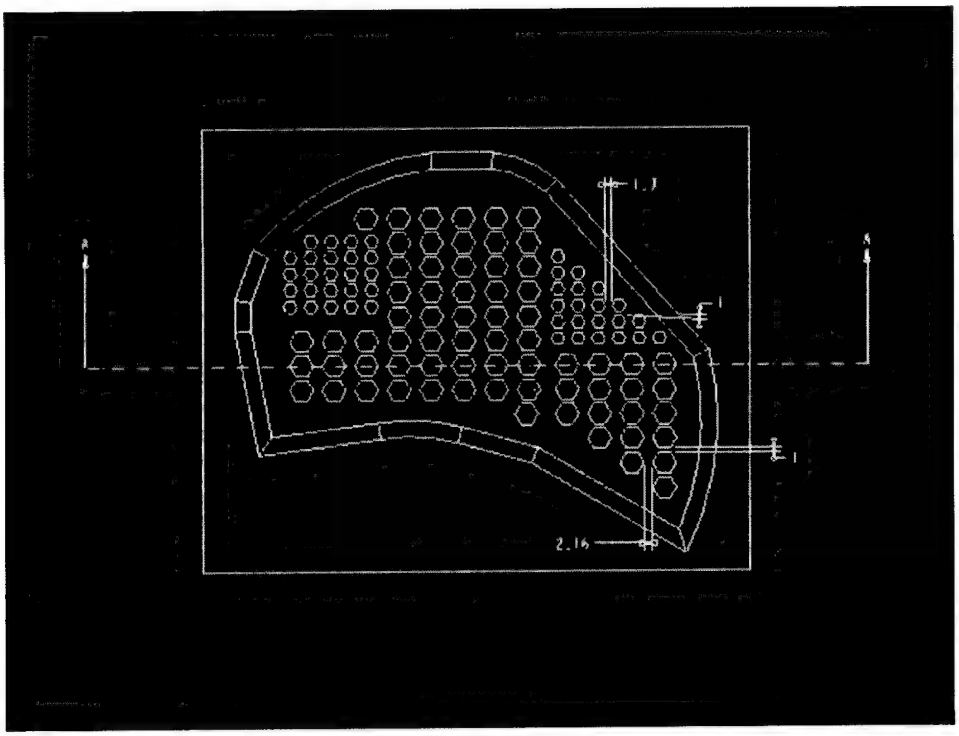

(a)

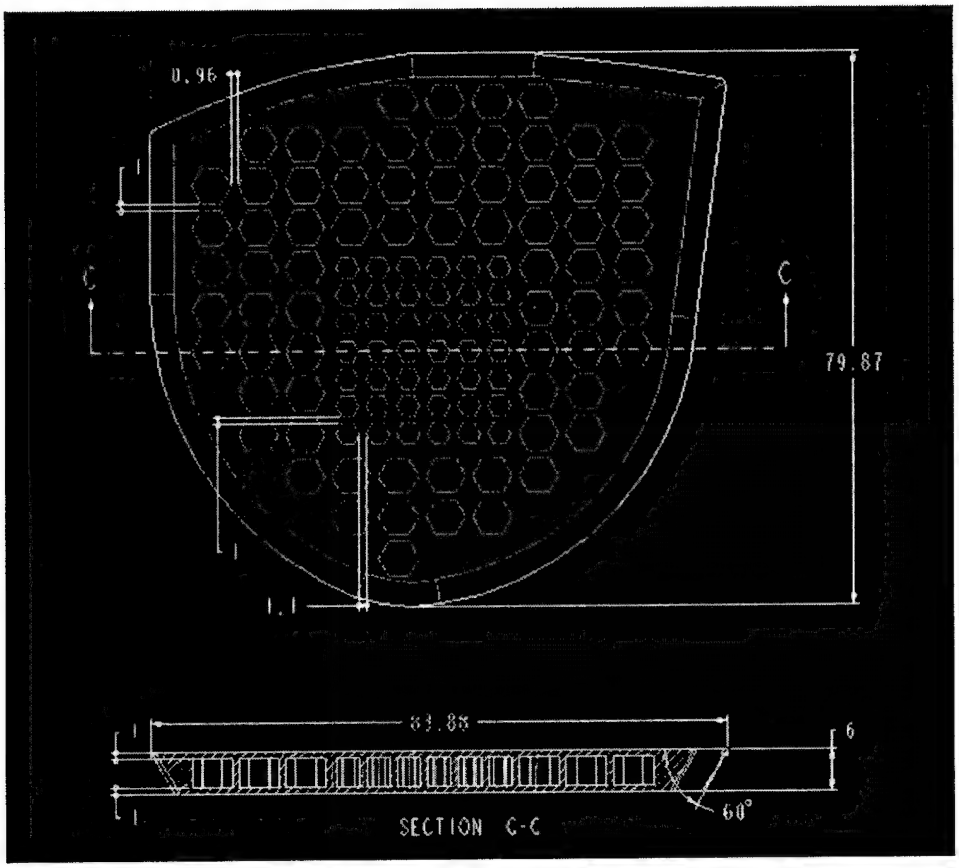

(b)

Figure 28. Initial design for **(a)** metatarsal head, and **(b)** heel cushions to be incorporated in the outer soles of footwear for treatment of metatarsalgia, plantar fasciitis, and heel spurs. As seen in Figure 26, the design mimics the anatomical structure of the pedal plantar fat pad, incorporating sealed, "honey comb" like septae, which serve as miniature hydraulic/pneumatic damping cylinders that dissipate and disperse locally applied loads.

Table 1. VA OSS ORTHOPEDIC SHOE LAST SURVEY MODIFICATION CODE LOG

	LAST REGION	MOD CODE	MAGNITUDE AND/OR DIRECTION OF MODIFICATION		LAST REGION		MAGNITUDE AND/OR DIRECTION OF MODIFICATION
1	TOE BOX AREA	A	RAISED 0 TO 1/4" DORSAL	6	FOREFOOT POSITION	A	ADDUCTED
		B	RAISED 1/4 TO 1/2" "			B	ABDUCTED
		C	RAISED 1/2/ TO 1" "			C	BUNION SHAPE
		D	WIDER WIDTH 0 TO 1/4 "			D	STRAIGHT
		E	WIDER WIDTH 1/4 TO 1/2 "				
		F	WIDER WIDTH 1/2 TO 1"	7	TONGUE/VAMP	A	BUILDUP 0 TO 1/4 "
		G	ADDITION TO PLANTAR AREA 0 TO 1/4 "			B	BUILDUP 1/4 TO 1/2 "
		H	ADDITION TO PLANTAR AREA 1/4 TO 1/2"			C	BUILDUP 1/2 TO 1 "
		I	ADDITION TO PLANTAR AREA 1/2 TO 1"				
				8	HEEL AREA	A	PLANTAR AREA DEPRESSION 0 TO 1/4 "
2	HALLUX AREA	A	RAISED DORSAL 0 TO 1/4 "			B	PLANTAR AREA DEPRESSION 1/4 TO1/2 "
		B	RAISED DORSAL 1/4 TO 1/2 "			C	PLANTAR AREA DEPRESSION 1/4 TO 1 "
		C	RAISED DORSAL 1/2 TO1 "			D	PLANTAR AREA RAISED 0 TO 1/4 "
		D	WIDEN AREA 0 TO 1/4 " MED SIDE			E	PLANTAR AREA RAISED 1/4 TO1/2 "
		E	WIDEN AREA 1/4 TO 1/2 " MED SIDE			F	PLANTAR AREA RAISED 1/2 TO 1 "
		F	WIDEN AREA 1/2 TO 1 " MED SIDE			G	LATERAL WEDGE 0 TO 1/4"
		G	PLANTAR AREA RAISED 0 TO 1/4 "			H	BUILDUP AROUND HEEL M/L 1/4"
		H	PLANTAR AREA RAISED 1/4 TO1/2 "				
		I	PLANTAR AREA RAISED 1/2 TO 1 "	9	HEEL POSITION	A	STRAIGHT
						B	INVERSION
3	5TH TOE AREA	A	RAISED DORSAL 0 TO 1/4 "			C	EVERSION
		B	RAISED DORSAL 1/4 TO 1/2 "				
		C	RAISED DORSAL 1/2 TO1 "	10	PLANTAR SURFACE	A	RAISE UNDER TOES (S,M,L)
		D	WIDEN AREA 0 TO 1/4 " LAT SIDE			B	RAISE UNDER METHEADS (S,M,L)
		E	WIDEN AREA 1/4 TO 1/2 " LAT SIDE			C	DEPRESSION UNDER TOES (S,M,L)
		F	WIDEN AREA 1/2 TO 1 " LAT SIDE			D	DEPRESSION UNDER METHEADS (S,M,L)
		G	PLANTAR AREA RAISED 0 TO 1/4 "			E	WEDGE LATERAL SIDE OF FOOT (S,M,L)
		H	PLANTAR AREA RAISED 1/4 TO1/2 "			F	WEDGE MEDIAL SIDE (S, M, L)
		I	PLANTAR AREA RAISED 1/2 TO 1 "			G	(S) 1/4SMALL , (M) 1/2MED (L) 3/4 LARGE
						H	OTHER THAN ABOVE
4	METATARSAL AREA	A	PLANTAR AREA DEPRESSION 0 TO 1/4 "				
		B	PLANTAR AREA DEPRESSION 1/4 TO1/2 "	11	ANKLE	A	BUILDUP MED 0 TO 1/2"
		C	PLANTAR AREA RAISED 0 TO 1/4 "			B	BUILDUP LAT 0 TO 1/2"
		D	PLANTAR AREA RAISED 1/4 TO1/2 "			C	BUILDUP BILATERALLY 0 TO 1/2"
						D	BUILDUP > 1/2" M(MED, L(LAT) B(BOTH)
5	ARCH AREA	A	PLANTAR AREA DEPRESSION 0 TO 1/4 "				
		B	PLANTAR AREA DEPRESSION 1/4 TO1/2 "				
		C	PLANTAR AREA DEPRESSION 1/4 TO 1 "				
		D	PLANTAR AREA RAISED 0 TO 1/4 "				
		E	PLANTAR AREA RAISED 1/4 TO1/2 "				
		F	PLANTAR AREA RAISED 1/2 TO 1 "				

Table 2. Female Test Subjects — Foot/Ankle Measurements (mm)

Sub No	Body H	Calf C	Heel Toe L	Heel Ball L	Heel Ant. Ankle L	Heel Lever	Toe Lever	Ball W Horiz	Ball W Dia	Heel to 5MTH	Heel W	Ball C	Waist C	Heel to Instep L	Instep C	Span C	Heel Toe Semi-C	Max Toe H	Ankle H	Ankle AP W	Ankle ML W	Ankle C	Malle-olus L-R	M Malle-olus H	L Malle-olus H	Dorsal Foot H	M Plan Arch H
1	168	37	24.5	17	10.5	6.2	17.3	9.5	10.5	16.2	7.37	26.9	26.5	10.5	29	34.5	27	3	10	9.37	6.8	26.5	6.9	8.5	7	7.8	1.85
2	178	30	25.8	18.3	9.3	6	20	9.6	10.1	17.5	6.3	24.4	24	11	24.1	34	28	2.6	11	8.9	7	24.3	6.8	9	7.8	7.6	4
3	160	27	24	17.5	8	4.6	18.5	8.9	9	16.1	6.2	20.6	21.5	9.5	21.8	30.8	25.7	2.5	9.28	7.1	6.2	19.4	6.6	7.83	6.13	6.62	2.3
4	164	28	22.6	17.1	8	5.7	16.9	8.1	8.2	14.36	5.9	21	19.7	11	20.4	29	25	2.2	9.1	7.3	5.3	19.7		7.28	5.58	5.89	2.86
5	161	32	24.2	17.4	8.6	4.5	19.7	9.2	9.53	14.14	6.1	24.5	22.8	10.1	24	31.3	25.3	2.3	10.46	8.2	5.4	21.9	6.7	7.7	6.68	6.54	2.68
6	159	32	23	16.5	10	5.1	13	9.1	9.5	14	6.4	23	23.1	10.6	24.2	31.1	26	2.7	10	7.6	6.1	21.2	6.2	8.25	7.4	7.3	2.6
7	155	38	23.2	17.3	10.5	6.5	16.7	9.6	10	14.5	5.8	23.6	23.8	12	24.1	31.9	25.6	2.8	9.7	8.1	7	23.3	6.7	8.38	6.84	7.22	4
8	157	31	22.9	16.7	9	4.5	18.4	8.2	8.9	14.5	5.9	21.1	20.7	11	21.8	30.3	26.2	2.8	8.54	7	5.6	20.9	6	7.28	6.4	6.51	2.89
9	157	34	23.6	16.9	8.5	4.7	18.6	8.9	9.1	14.7	5.7	21.2	21.1	11.4	22	31.2	25.6	2.8	10.3	6.7	5.2	19.8	5.8	8.77	6.55	7.22	3.41
10	171	30	23.4	17.1	7.7	5.7	17.7	8.5	8.6	15.6	5.2	21.3	20.7	9.3	21.9	31.5	26.5	2.4	10.75	6.5	4.9	19.8	6.4	8.63	6.8	6.99	3.65
11	165	32	25	18.4	8.8	5.4	19.6	9	9.1	16.6	5.9	22.1	21.9	10	22.9	31.4	31.4	2.4	10.18	6.6	5.5	20.3	6.8	8.24	6.98	6.47	3.13
12	154	32	22.8	17.1	9	5.5	17.3	8	8.2	14.9	5.5	20	19.8	9.9	21.9	28.4	25.5	2.2	9.43	6.8	5.2	19.7	6	7.38	6.61	6.15	3.05
13	163	33	24.1	17.4	9	5	15	8.8	8.9	15.5	6.1	22.1	22.5	11	23.4	32.4	27.1	2.7	10.4	6.8	6	20.5	6.1	8.08	7.1	7	3.35
14	165	30	22.6	17	8.5	5.5	17.1	8	8.1	14.3	5.1	20	20.4	10.4	20.5	31.1	25.6	2.5	10.3	6.6	5	19.1	5.8	7.86	6.2	6.1	2.73
15	160	33	22.6	16.9	7.8	6.3	16.3	8.3	8.6	14.4	5.5	21.6	21.4	9.9	22.8	30.3	25.7	2.1	9.71	6.5	5.5	20.1	6.4	7.42	6.53	6.46	2.8
16	173	38	25.9	19.4	10	6.4	19.5	9.6	9.8	17.1	6.5	24.5	25	11.6	25.1	36.8	29.1	3.7	12.03	7.9	6.1	23.6	7	9.67	7.62	7.03	3.36
17	165	29	24.7	18.1	10	6.3	18.4	9	9.1	16.4	6.8	22.9	22.7	12.3	23	33.9	29.2	3.1	9.95	7.6	5.6	21.3	6.3	8.43	6.87	6.84	3.06
18	160	31	22.6	16.4	8.5	5.5	17.1	9.3	9.4	14.5	5.5	22.1	21.1	10.6	21.8	30.9	25.1	2	9.3	6.4	5.1	19	6	7.3	6.53	6.04	2.1
19	165	32	24.9	17.8	9	5.5	19.4	9.6	9.3	15.5	6.2	23.1	23	11	23.6	31.6	27.1	2.6	9.91	7.5	5.8	21.7	6.3	8.17	6.92	6.69	2.43
20	173	32	24.5	18.2	9.7	6	18.5	8.9	9.2	15.4	6.5	23	22.3	11.6	24	34.3	26.6	3.2	10.53	7.8	6.2	22.8	6.3	8.58	7	7.5	3.88
21	152	35	22.5	16.2	8.7	5.2	17.3	8.9	9	13.8	5.7	23.4	22.8	9.6	23.9	31.3	24.5	2.9	10.33	7.5	5.9	21.8	6.8	8.32	6.66	7.01	3.06
22	163	37	23.7	17.6	8.8	6	17.7	8.7	8.8	14.9	6	22.7	22.4	11.5	23.4	33.2	27	2.5	10.84	8.5	6.6	24.5	6.5	8.97	6.76	7.2	3
23	160	32	24	17.9	8.9	6.4	17.6	8.6	8.9	15.2	5.8	22	21.6	10.9	23	32.7	26.9	2.9	10	7.1	5.4	21	6.3	7.67	7.23	7.28	2.3
24	175	32	25.4	18.5	9.6	6.4	19	9.2	9.3	16.6	5.7	23.4	22.5	12.5	23.5	32.4	27.7	2.4	10.94	7.5	5.4	21.3	7.3	8.58	6.49	7.16	2.29
25	161	31	24.5	17.8	8.2	6	18.5	9.1	9.5	14.5	6.5	22.6	22.6	12	24.1	33.9	27.3	2.7	10.86	7.3	5.2	21	6	8.59	6.36	7.58	2.8
26	171	40	25.4	19.7	9.4	7.6	17.8	10.2	10.4	16.6	7.6	25.9	26.7	12.9	26.6	35.8	29.5	3.7	10.2	8.6	6.8	25.4	7.5	8.03	7.07	6.73	1.51
27	157	34	23.4	17.4	8.6	5.6	17.8	9.7	9.8	14.6	5.5	23.7	22.3	10.7	23.2	32.8	27	2.8	10.9	7.6	5.9	21.5	6.4	8.3	7.39	7.5	3.48
28	165	29	24.8	18.1	7.8	4.9	19.9	8.9	9	16.1	5.5	22	22.4	10.7	23.9	32.2	27.3	2.2	9.9	6.9	5.5	20.3	6.6	7.59	7.31	6.83	1.56
29	171	27	26.5	19.6	10.5	7.4	19.1	9.5	9.8	17.6	7.3	25	25	13.1	26.3	38.8	30.8	2.8	11	7.5	5.6	21.8	6.6	9.12	7.07	8.36	3.22
30	168	32	24.6	18	7.1	5.5	19.1	9.2	9.3	15.4	6.2	23.4	22.7	11.9	24.5	33.6	28.1	2.6	10.8	7.7	6.5	22.8	6.6	9.1	7.73	7.65	3
31	165	31	24.4	17.6	8.6	6.4	18	8.8	8.9	15.6	6	22.8	22.2	11.8	23	31.2	27.1	2.8	9.9	7.5	5.8	21	6.8	8.3	6.79	7.18	2.69
32	160	29	23.8	17.8	8.8	5.9	17.9	9.2	9.3	15	6.3	22.1	22	10.5	22.8	31.5	26	2.3	9.68	6.9	5.9	20.8	6.5	7.88	7.56	6.56	2.05
33	157	34	22.6	16.6	7.8	5.9	16.7	8.9	9.1	13.4	6.4	22.5	22	10.9	22.7	30.3	26.1	2.6	9.28	6.8	5.6	20.5	6.3	7.55	5.88	6.29	2.56
34	157	36	22.5	16	8.1	5.5	17	8.7	8.9	13.9	5.2	22.3	22	10.4	22	30.1	24.6	2.4	9.83	7.1	5.4	20.1	6.6	7.98	6.5	7.03	2.65
35	165	32	24.8	18.1	9.8	6.5	18.3	8.5	8.9	15	5.7	33.5	22	10.9	25	32.1	26	2.3	10.5	7.5	5.1	19.9	6.5	8.5	6.78	7.79	2.96
36	163	34	24.3	18.2	9.8	7.7	1.6	9.4	9.5	15	6.7	24.5	25	11	24.1	33.1	27.5	3.6	11.53	8	5.8	28	7.11	9.32	7.83	7.5	2.37
37	168	29	24.2	17.6	8.1	5.5	18.9	8.8	8.9	15.5	5.8	22.4	21	11.4	23.2	37.1	26.8	2.3	9.81	6.7	5.2	20.1	6.1	7.98	6.46	6.5	2.53
38	163	36	26.1	19.3	6.5	7	19.1	9.7	10.1	17.1	6.7	24.3	24.7	11	28	34.9	29.2	2.4	9.37	8.3	6.4	24.8	7.1	7.87	6.9	7.4	2.73
39	157	26	22.6	16.6	8.2	4.3	18.9	8	8.2	14	4.9	20.4	19.6	9.5	21	27.9	25.2	2.1	9.26	5.8	4.6	17.2	6.1	7.28	7.14	5.96	2.83
40	173	29	25.8	19.1	10	6.5	19.3	9.5	9.6	15.5	6.3	22.5	22.7	11	25	32.3	28.1	2.4	9.05	7.3	5.4	20.5	6.7	7.23	5.62	6.89	2.31
41	162	35	24.7	18.4	10	6	18.7	8.9	9	15.3	6.1	23	21.3	11	22.8	31	26.2	2.6	11.6	6.8	5.5	21.7	6.2	9.07	6.62	7.65	2.94
42	156	33	22.2	16.5	7.4	5.6	16.6	8.6	8.7	13	5.8	21.8	20.8	10.5	22	30.2	25.9	2	11	6.2	5.1	19	6.1	7.8	7.3	6.53	3.35
43	169	26	25.7	19.1	9.9	5.5	20.2	8.9	9	16	6.3	20	22.6	12.6	23	32	29	2.9	11.2	6.9	5.4	20.4	6.5	8.26	6.97	6.71	3.52

H = height L = length W = width C = circumference

Table 3. Optimization of Pedorthic Treatment for Podalgia

Stresses–Strains in Heel Pad Soft Tissue vs Pedorthic Insole Stiffness & Geometry

Pedorthic Insole	Heel Pad Maximum Cauchy Stress (*MPa*)	Heel Pad Maximum Green Strain (*mm/mm*)	Heel Pad Maximum Strain Energy Density ($x10^{-3}$ *Joule / mm*^{3})
(a) No Insole	–0.412	–0.459	53.06
(b) Standard flat insole with 1x stiffness of heel pad tissue	–0.354	–0.445	33.77
(c) Standard flat insole with 2.5 x stiffness of heel pad tissue	–0.378	–0.452	40.90
(d) Standard flat insole with 6 x stiffness of heel pad tissue	–0.394	–0.455	46.27
(e) Standard flat insole with 6 x tissue stiffness & 25mm base diameter 2.5mm deep conical relief on bottom surface	–0.342	–0.438	30.44
(f) Standard flat insole with 6 x tissue stiffness & 25mm base diameter 2.5mm deep conical relief on top surface	–0.341	–0.436	30.06
(g) Standard flat insole with 6 x tissue stiffness & 20mm diameter cylindrical relief	–0.277	–0.400	13.08
(h) Standard flat insole with 6 x tissue stiffness & 14mm diameter cylindrical relief	–0.344	–0.434	30.87
(i) Custom contoured insole with 6 x tissue stiffness & 14mm diameter cylindrical relief	–0.236	–0.384	8.91
(j) Custom contoured insole with 2.5 x tissue stiffness & 14mm diameter cylindrical relief	–0.234	–0.381	8.84
(k) Custom contoured insole with 6 x tissue stiffness, 20mm diameter cylindrical relief	–0.197	–0.344	5.76
(l) Custom contoured insole with 6 x tissue stiffness, 25mm base diameter 2.5mm deep conical relief on top surface	–0.222	–0.373	7.80
(m) Custom contoured insole with 6 x tissue stiffness, 14mm diameter cylindrical relief, & constrained tissue movement	–0.167	–0.252	13.51
(n) Custom contoured insole with 2.5 x tissue stiffness, 14mm diameter cylindrical relief, & constrained tissue movement	–0.171	–0.249	14.47
(o) Custom contoured insole with 6 x tissue stiffness, 20mm diameter cylindrical relief, & constrained tissue movement	–0.172	–0.256	14.06
(p) Custom contoured insole with 6 x tissue stiffness, 25mm base diameter 2.5mm deep conical relief on top surface, & constrained tissue movement	–0.168	–0.254	13.52
(q) Custom contoured insole with 6 x tissue stiffness, 25mm base diameter 3 mm deep conical relief on bottom surface, & constrained tissue movement	–0.169	–0.254	13.69
(r) Custom contoured insole with 2.5 x tissue stiffness, 25mm base diameter 3 mm deep conical relief on bottom surface, & constrained tissue movement	–0.170	–0.250	14.36

Table 4. Optimization of Pedorthic Treatment for Vertical Calcaneal Osteophyte Stresses–Strains in Heel Pad Soft Tissue vs Pedorthic Insole Stiffness & Geometry

Pedorthic Insole	Heel Pad Maximum Cauchy Stress *(MPa)*	Heel Pad Maximum Green Strain *(mm/mm)*	Heel Pad Maximum Strain Energy Density *($x10^{-3}$ Joule / mm^3)*
(a) No Insole	–6.538	–0.497	822.9
(b) Standard flat insole with 1x stiffness of heel pad tissue	–5.160	–0.4916	529.0
(c) Standard flat insole with 2.5 x stiffness of heel pad tissue	–5.808	–0.495	671.7
(d) Standard flat insole with 6 x stiffness of heel pad tissue	–6.170	–0.496	748.8
(e) Standard flat insole with 6 x tissue stiffness & 25mm base diameter 2.5mm deep conical relief on bottom surface	–4.634	–0.486	430.2
(f) Standard flat insole with 6 x tissue stiffness & 25mm base diameter 2.5mm deep conical relief on top surface	–4.544	–0.486	415.0
(g) Standard flat insole with 6 x tissue stiffness & 20mm diameter cylindrical relief	–2.796	–0.458	216.5
(h) Standard flat insole with 6 x tissue stiffness & 14mm diameter cylindrical relief	–4.563	–0.485	423.8
(i) Custom contoured insole with 6 x tissue stiffness & 14mm diameter cylindrical relief	–2.270	–0.445	160.1
(j) Custom contoured insole with 2.5 x tissue stiffness & 14mm diameter cylindrical relief	–2.186	–0.440	152.8
(k) Custom contoured insole with 6 x tissue stiffness, 20mm diameter cylindrical relief	–1.470	–0.3972	72.3
(l) Custom contoured insole with 6 x tissue stiffness, 25mm base diameter 2.5mm deep conical relief on top surface	–1.946	–0.4353	119.5
(m) Custom contoured insole with 6 x tissue stiffness, 14mm diameter cylindrical relief, & constrained tissue movement	–0.351	–0.252	13.4
(n) Custom contoured insole with 2.5 x tissue stiffness, 14mm diameter cylindrical relief, & constrained tissue movement	–0.318	–0.249	14.5
(o) Custom contoured insole with 6 x tissue stiffness, 20mm diameter cylindrical relief, & constrained tissue movement	–0.184	–0.256	14.0
(p) Custom contoured insole with 6 x tissue stiffness, 25mm base diameter 2.5mm deep conical relief on top surface, & constrained tissue movement	–0.317	–0.254	13.5
(q) Custom contoured insole with 6 x tissue stiffness, 25mm base diameter 3mm deep conical relief on bottom surface, & constrained tissue movement	–0.304	–0.254	13.7
(r) Custom contoured insole with 2.5 x tissue stiffness, 25mm base diameter 3mm deep conical relief on bottom surface, & constrained tissue movement	–0.391	–0.264	14.3